

Original Research

Immune Imbalance in Primary Membranous Nephropathy at Single-cell Resolution

Xuan Tie^{1,2,3,†}, Zhiang Chen^{4,†}, Shulei Yao^{1,2,3,†}, Binxin Wu^{1,2,3}, Bingjuan Yan^{1,2,3}, Huifang Zhai^{1,2,3}, Xi Qiao^{1,2,3}, Xiaole Su^{1,2,3,*}, Lihua Wang^{1,2,3}

Submitted: 13 December 2024 Revised: 17 January 2025 Accepted: 25 January 2025 Published: 24 February 2025

Abstract

Background: Primary membranous nephropathy (pMN) often progresses to end-stage renal disease (ESRD) in the absence of immunosuppressive therapy. The immunological mechanisms driving pMN progression remain insufficiently understood. Methods: We developed a single-cell transcriptomic profile of peripheral blood mononuclear cells (PBMCs) from 11 newly-diagnosed pMN patients and 5 healthy donors. Through correlation analysis, we identified potential biomarkers for disease stratification and poor prognosis. Results: Expression levels of several proinflammatory factors were significantly increased in patients compared to healthy donors, such as interleukins (IL1B, IL8, and IL15) and interferon G (IFNG). Multiple pattern recognition receptors involved in proinflammatory signaling were also upregulated in patients, including NOD-like receptors (NLRs) (NLRP1, NLRP3, and NLRC5), RNA helicases (DDX58, IFIH1, DHX9, and DHX36), cGAS (cyclic GMP-AMP synthase) and IFI16 (interferon gamma inducible protein 16). Additionally, human leukocyte antigen molecules HLA-DQA1 and HLA-DRB1 enriched in memory B cells were upregulated in patients. More importantly, we found that the genes for antiviral defense response were significantly elevated in high-risk patients relative to the low-risk group. More than twenty genes were negatively correlated with estimated glomerular filtration rate (eGFR), such as BST2 (bone marrow stromal cell antigen 2) and SLC35F1 (solute carrier family 35 member F1). Their predicted values were confirmed in a larger population with nephrotic syndrome or other chronic kidney diseases from a public database. Furthermore, we developed a series of scoring systems for distinguishing high-risk patients from low- and moderate-risk individuals. Conclusions: Our study provides insight into the immunological mechanism of pMN and identifies numerous biomarkers and signaling pathways as potential therapeutic targets for managing the progression of high-risk pMN.

Keywords: primary membranous nephropathy (pMN); single-cell RNA sequencing; peripheral blood mononuclear cells (PBMCs); immune imbalance; biomarkers

1. Introduction

Membranous nephropathy (MN) is a pathologically diagnosed disease of the kidney glomerulus, which is the leading cause of nephrotic syndrome in adults [1]. The morphological feature of MN is the presence of immune deposits in the subepithelial space of the glomerular filtration barrier. The immune deposits consist of the relevant antigens, autoantibodies and complement components, which might trigger an inflammatory response, leading to further damage and increased permeability of the glomerular basement membrane (GBM) [2]. Proteinuria and generalized edema are major clinical manifestations of MN. Patients with MN may have also other concurrent diseases, such as other autoimmune disorders, malignancies or infections. These patients are often diagnosed as secondary MN (sMN). Those without identifiable underlying cause are considered to be primary MN (pMN) [3]. In our study,

we focus on newly-diagnosed pMN with circulating autoantibodies against the phospholipase A2 receptor 1 (PLA2R1) [4].

Prognosis of pMN is highly variable. Among patients with persistent nephrotic syndrome, 40 to 50% of them will progress into end-stage renal disease (ESRD) within 10–15 years, in part due to an incomplete understanding of its pathogenic mechanism [1]. Recent studies attempted to elucidate the underlying mechanisms of pMN using single-cell RNA sequencing of kidney biopsy tissues [5–7]. However, due to few immune cells in these tissues, it remains unclear about immune abnormalities in patients with newly diagnosed pMN, especially in those at high risk. Despite two study analyzed B cells from patients with pMN, only three blood samples with PBMCs were included [8,9]. No comprehensive single-cell immune profile of adult with pMN has been reported to date.

¹Department of Nephrology, Second Hospital of Shanxi Medical University, 030000 Taiyuan, Shanxi, China

 $^{^2 {\}rm Shanxi}$ Kidney Disease Institute, 030000 Taiyuan, Shanxi, China

 $^{^3}$ Institute of Nephrology, Shanxi Medical University, 030000 Taiyuan, Shanxi, China

⁴Zhejiang University School of Medicine, 310058 Hangzhou, Zhejiang, China

^{*}Correspondence: Kunle6609@163.com (Xiaole Su)

[†]These authors contributed equally. Academic Editor: Vesna Jacevic

Peripheral blood contains a large number of immune cells, making it ideal for mapping the single-cell immune landscape of patients with pMN. In our study, we identified a series of high-expression genes in high-risk patients compared to low-risk population, which plays a critical role in antiviral defense response. Meanwhile, we found a set of novel biomarkers for distinguishing patients from healthy donors.

2. Materials and Methods

2.1 Patients and Samples

In this study, we included 11 patients with newly diagnosed pMN, all of whom had circulating autoantibodies against phospholipase A2 receptor 1 (PLA2R1). None of the patients had a history of other diseases or treatment of steroids and immunosuppressive drugs in the past year. One patient refused to undergo kidney biopsy. Based on the KDIGO 2021 guideline for the management of glomerular diseases [10], the patients were categorized into three groups: low-risk group (3 patients), moderate-risk group (4 patients) and high-risk group (4 patients).

Peripheral venous blood samples were collected from patients before treatment. PBMCs were isolated using density gradient centrifugation with Ficoll-Paque from 5 milliliter fresh anticoagulated blood. The isolated cells were resuspended in cryopreservation medium [900 μ L of fetal bovine serum supplemented with 100 μ L of dimethyl sulfoxide (DMSO)] for long-term storage liquid nitrogen.

2.2 Single-Cell RNA Library Preparation and Sequencing

Cryopreserved PBMCs from all patients were thawed, and cell viability was assessed, consistently exceeding 90%. Single-cell suspensions containing 10,000 to 20,000 cells were loaded for library construction using the Chromium Single Cell 3' Library ($10\times$ Genomics, Inc., Pleasanton, CA, USA) following the manufacturer's protocol. The quality of the purified libraries was evaluated, and sequencing was performed on an Illumina NovaSeq X Plus platform (Illumina, Inc., San Diego, CA, USA) using 150-bp pairedend reads.

2.3 Single-Cell RNA-seq Data Processing

We performed single-cell RNA sequencing (scRNA-seq) on PBMCs from 11 patients with pMN and integrated a published scRNA-seq dataset from 5 healthy donors as a control group [11]. Samples were stratified into four groups correspondingly: normal (healthy donors), low (low-risk patients), moderate (moderate-risk patients), and high (high-risk patients). Raw sequencing data were processed using the Cell Ranger Software Suite 7.1.0 (10× Genomics, Inc., Pleasanton, CA, USA), aligning reads to the human reference genome (refdata-gex-GRCh38-2020-A). Filtered count matrices were imported into Seurat 4.3 (https://satijalab.org/seurat/) for downstream analysis. Quality control criteria included: 500–5000 detected genes per cell,

total unique molecular identifier (UMI) count \leq 20,000, and mitochondrial gene expression \leq 10%. Doublets were identified and removed using DoubletFinder 2.0.3 (https://github.com/chris-mcginnis-ucsf/DoubletFinder). The cleaned data were normalized and scaled using Seurat's built-in functions.

2.4 Batch Effect Correction and Cell Type Annotation

To integrate cells from different individuals and risk levels, we employed Harmony 1.2 (https://github.com/imm unogenomics/harmony) to correct batch effects and create a shared embedding [12–15]. Dimensionality reduction and clustering were performed using 2000 highly variable genes and 30 principal components. Marker genes for each cluster were identified using Seurat's FindAllMarkers function with default parameters. Initial cell type annotation was performed using CellTypist 1.6.3 (https://www.celltypist.org/) with the 'Immune_All_Low.pkl' model [16], followed by manual refinement based on known marker genes from the literature.

2.5 Differential Expression and Enrichment Analysis

To explore the differences between disease and control groups, we identified differentially expressed genes (DEGs) for each cell type using Seurat's FindMarkers function, comparing patients (different risks) with healthy donors. Genes with |log2FC| ≥0.5 and adjusted *p*-value ≤ 0.05 were considered significant DEGs. Gene Ontology (GO) and Kyoto Encyclopedia of Genes and Genomes (KEGG) pathway enrichment analyses were performed using the clusterProfiler 4.6.2 (https://github.com/YuLab-SMU/clusterProfiler) package with default parameters to elucidate the biological processes and pathways associated with the identified DEGs.

2.6 Gene Set Signature Scoring and Comparison

To assess the expression of specific gene sets, we utilized Seurat's AddModuleScore function to calculate signature scores for each cell [13]. Comparisons of signature scores among different disease and control groups were performed using analysis of variance (ANOVA) and the Kruskal-Wallis test to identify statistically significant differences.

2.7 Cell-Cell Interaction Analysis

To predict cell-cell communication, we employed CellChat 1.6.1 (https://github.com/sqjin/CellChat) to analyze ligand-receptor pairs [17]. Interaction strength was calculated for individual ligand-receptor pairs between each pair of cell types and aggregated to determine the overall interaction strength of signaling pathways. Comparative analyses were performed between disease groups (low, medium, and high risks) and the control group to identify alterations in cell-cell communication associated with disease progression. Significant signaling pathways were cal-



Table 1. Baseline characteristics of patients with pMN.

	P1	P2	Р3	P4	P5	P6	P7	P8	P9	P10	P11
Gender (F/M)	M	F	F	F	F	F	F	F	F	F	M
Age (years)	67	49	39	59	30	40	27	41	36	56	44
Generalized edema	yes	yes	yes	yes	yes	yes	yes	yes	yes	yes	yes
MN stage	II	III	II	II	I–II	II	II–III	II	II	II	I
Anti-PLA2R1 (RU/mL)	258.3	37.3	211.0	373.1	2.5	159.1	100.6	160.2	71.1	27.8	51.9
Serum albumin (g/L)	25.4	25.0	34.6	25.0	34.7	30.0	27.7	31.5	30.3	33.1	31.5
Urinary protein (g/24 hours)	6.8	6.4	7.3	6.0	4.3	7.1	4.7	4.3	2.7	1.6	2.8
Serum creatinine (umol/L)	116	75	58	61	66	62	58	45	65	49	60
eGFR (mL/min/1.73 m ²)	55.8	80.6	111.5	95.3	107.5	108.1	121.3	119.5	105.0	104.6	116.2
IgG4 deposition	2+	2+	2+	2+	2+	2+	3+	3+	2+	3+	3+
IgG3 deposition	-	-	\pm	-	-	1+	1+	-	-	-	-
IgG2 deposition	-	-	-	-	-	-	2+	2+	-	-	-
IgG1 deposition	-	-	-	-	\pm	-	2+	2+	1+	1+	-
IgA deposition	1+	-	-	-	-	-	1+	-	3+	-	-
IgM deposition	1+	\pm	1+	\pm	\pm	\pm	2+	1+	2+	-	\pm
C3 deposition	1+	1+	2+	2+	1+	1+	1+	-	1+	-	1+
C1q deposition	1+	1+	-	1+	-	\pm	-	-	1+	-	-
PLA2R staining	3+	2+	2+	3+	2+	3+	3+	3+	2+	2+	3+
Risk stratification	high	high	high	high	moderate	moderate	moderate	moderate	low	low	low
Crescent formation	0/45	0/24	0/20	0/19	0/16	0/13	0/12	0/64	0/9	0/27	0/33
Gromerular sclerosis	4/45	0/24	0/20	0/19	0/16	0/13	1/12	3/64	0/9	3/27	0/33
Tubularinterstitial injury (%)	5	< 5	< 5	< 5	<5	<5	15	<5	<5	5	<5
Interstitial infiltration (%)	<25	<25	<25	<25	<25	<25	<25	<25	<25	<25	<25
Prior therapy	no	no	no	no	no	no	no	no	no	no	no
Combined disease	no	no	no	no	no	no	no	no	no	no	no

P1-11, patient 1 to 11; F, female; M, male; eGFR, estimated glomerular filtration rate; MN stage, membranous nephropathy stage; Anti-PLA2R1, antibody against phospholipase A2 receptor 1.

culated and ranked based on differences in the overall information flow within the inferred networks between disease and control groups.

2.8 Statistical Analysis

All statistical analyses were performed using R 4.2.3 (https://www.r-project.org/). Differential expression testing was conducted using FindMarkers with the Wilcoxon Rank Sum test, and p-values were adjusted by the Bonferroni correction method. Enrichment analyses were performed using the clusterProfiler package with the permutation test, and p-values were adjusted by the Benjamini-Hochberg method. To assess the statistical significance of signature score changes observed in a given cell subtype among different groups, we employed Bonferroni's test for multiple comparison. To perform Pearson correlation analysis between candidate genes in high-risk patients and estimated glomerular filtration rate (eGFR), a linear regression model was applied to estimate the slope of the regression line and its 95% confidence interval. The data used for correlation analysis were from our own study and a public database Nephroseq v5 (https://nephroseq.org). An adjusted p-value < 0.05 was considered statistically significant and annotated above the box plot as follows: p < 0.05*, p < 0.01 **, p < 0.001 ***, and p < 0.0001 ****.

3. Results

3.1 Landscape of Peripheral Blood Mononuclear Cells Using Single-cell RNA Sequencing

Apart from the kidney biopsy tissue, peripheral blood mononuclear cells are also important for dissecting the immunological mechanism of pMN. Using the 10×Genomics scRNA-seq method, we obtained our own dataset from 11 patients (Fig. 1A), comprising 3 low-risk, 4 moderate-risk and 4 high-risk individuals. Anti-PLA2R1 antibodies were positive in all patients (Table 1). We compiled our data and a published one with 5 healthy individuals, which served as a negative control group (Supplementary Table 1). After stringent quality control and filtration, a total of 178,185 single-cell transcript data of PBMCs were analyzed. After correcting batch effects between the two datasets, we integrated the data to perform unsupervised graph-based clustering. Five major lineages (T cells, B cells, NK cells, Monocytes and cDC2) were identified depending on a referenced automatically annotation (Fig. 1B,D) [16]. In addition, other kinds of immune cells were not used to perform analysis due to their low abundance, including innate lymphoid cell 3 (ILC3), natural killer T cells (NKT), immature lymphoid cells and platelets and so on (Fig. 1B). The published data contained the same types of cells as ours. Cell annotations were verified independently by two investiga-



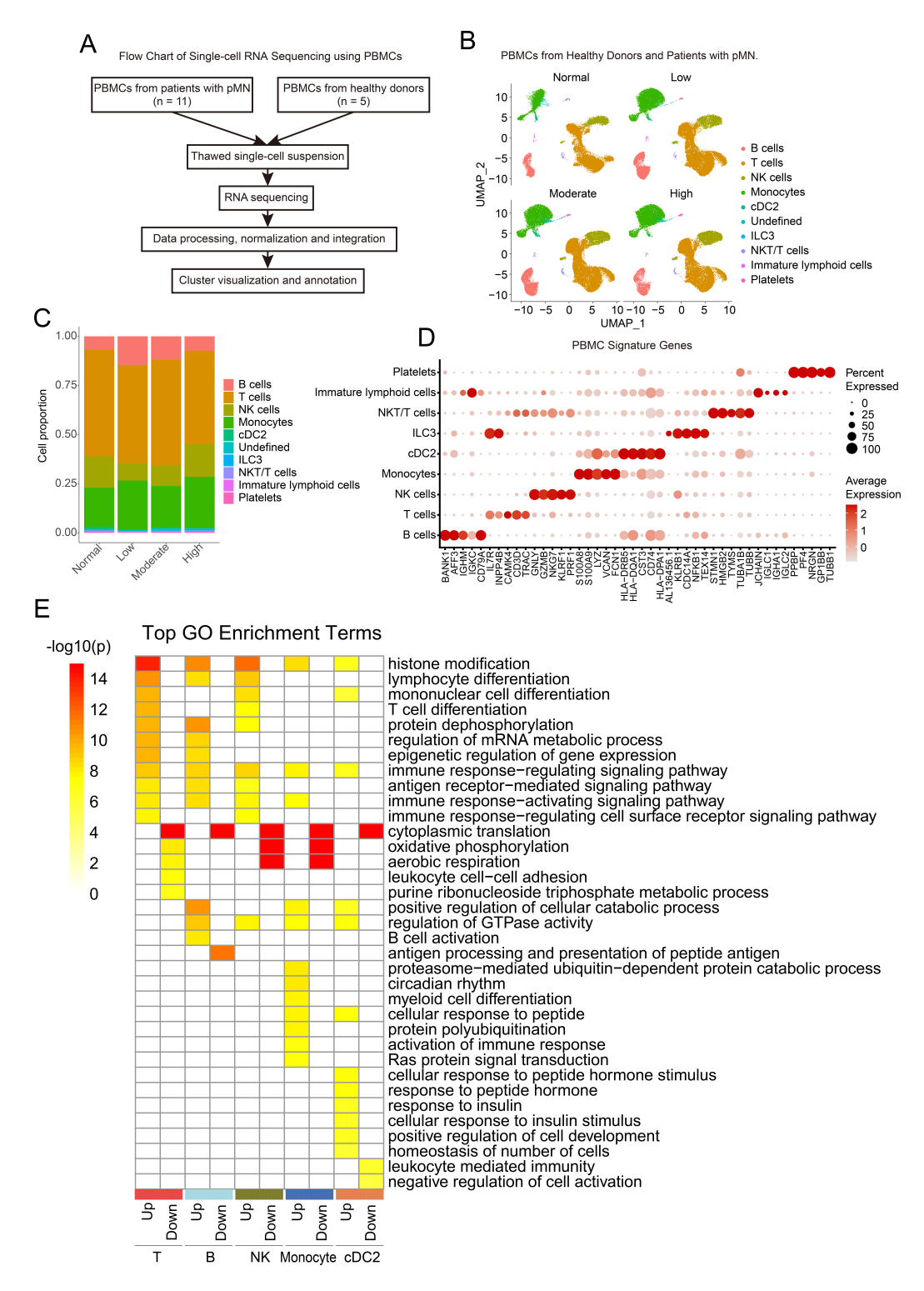


Fig. 1. Single-cell RNA analysis of PBMCs from individuals with pMN and healthy controls. (A) Overview of the participants included and samples and data collected. (B) UMAP visualization of the five cell clusters (T, B, NK, monocytes and cDC2) in the integrated single-cell transcriptomes of 178,185 cells derived from pMN and healthy donors, other cell clusters included innate lymphoid cell 3, NKT and T cells, immature lymphoid cells and platelets and so on. (C) Bar plot of the proportion of cell types shown in healthy controls (normal), low-risk (low), moderate-risk (moderate) and high-risk (high) patients with pMN. (D) Dot plot showing the expression of selected signature genes in each cluster. (E) Gene ontology (GO) assignments of top GO terms that were upregulated or downregulated in specific cell types from patients with pMN versus healthy control, respectively. PBMCs, peripheral blood mononuclear cells; pMN, primary membranous nephropathy; cDC2, classical dendritic cell 2; UMAP, uniform manifold approximation and projection; NKT, natural killer T cell.

tors to ensure accuracy. No significant differences were observed in the overall distribution of cell populations across the four groups (Fig. 1C).

We conducted GO enrichment analysis on the five kinds of immune cells, comparing patients with pMN to healthy donors. Top up-regulated and down-regulated signaling pathways were showed in individual type cells. Immune-response related pathways were notably more active in patients across all cell types (Fig. 1E). The average capacity of antigen presentation was reduced in B cells from patients (Fig. 1E).

In order to discovery more positive results, we decided to divided specific type of immune cells into several subtypes. Based on reference annotations, individual cell lineages were categorized as shown in Fig. 2. CD4+ T cells were divided into three subgroups, including naive T (Tn) and central memory T (Tcm), effector T (Te) and effector memory T (Tem) and regulatory T cells (Treg). CD8+ T cells were classified into three subgroups, including Tn and Tcm, Tem and Temra (CD45RA⁺), Tem and resident memory T cells (Trm) (Fig. 2A-C). B cells included naive (Bn), activated B (Ba), non-switched memory (Bnsm) and switched memory B cells (Bsm) (Fig. 2D-F). NK cells included CD56^{+/-} NK cells (or CD56^{dim}CD16^{high}) and CD56⁺ NK cells (or CD56^{bright}CD16^{low}) (Fig. 2G-I). Monocytes consisted of two subgroups, namely classical (CD14⁺CD16⁻) and nonclassical monocytes (CD14⁻CD16⁺) (Fig. 2J–L). Of note, classical dendritic cell 2 (cDC2) and MAIT did not subdivide further in our dataset (Fig. 1B).

3.2 Abnormal Expressions of Immunoglobulins and Components of Complement System

As we know, circulating immunoglobulin G4 (IgG4) are thought to bind to deposited autoantigens and form the subepithelial complex. To investigate the potential correlation between immunoglobulins and disease severity, we analyzed the data of B cells. From naive to memory B cells, expression levels of IGHD and IGHM gradually decreased, confirming that our data was qualified (Fig. 3A). Consistent with IgG4 deposition in glomerular biopsies, IGHG4 expression in memory B cells was higher in patients than in healthy donors (Fig. 3D). Similar trend was observed for IGKC (Fig. 3F). Intriguingly, transcript levels of IGHG3 in memory B cells were gradually upregulated from low-risk to high-risk patients (Fig. 3A,B). Whereas expression levels of IGHA1 and IGHG2 in activated and memory B cells were lower in patients (Fig. 3C,E). Together, these results suggest that IgG3 might participate into the progression of pMN with antibodies against PLA2R1 [18].

Complement activation plays a central role in the pathogenesis of pMN. Subepithelial deposition of circulating immune complexes promotes the formation of the terminal complement component C5b-9, which subsequently damaged the glomerular basement membrane (GBM) [18].

To determine whether the complement system was active in peripheral immune cells, we analyzed complement-related markers in B cells. We found that complement receptor 1 (CR1) expression in B cells was higher in patients compared to controls (Fig. 3G). Similar trend was showed in patients with regard to C1S, C2 and C5. To provide a more accurate assessment, we developed a score using a panel of biomarkers up-regulated in patients, including C1S, C2, C5, CR1, CD46, CD55 and ITGAX. Scores for memory B cells and monocytes were significantly higher in patients than in healthy donors (Fig. 3H). These findings indicate that abnormal activation of complement system was present in patients with pMN, potentially contributing to disease progression.

3.3 Activation of Proinflammatory Response in pMN

Chronic inflammation is a prominent feature of many autoimmune diseases [19], including pMN. Numerous proinflammatory pathways, involving interleukins, interferons, tumor necrosis factors, chemokines, growth factors and their corresponding receptors, may contribute to the development of pMN. Nevertheless, that the relationship between proinflammatory responses and pMN progression remains poorly understood. To address this issue, we investigated the expression levels of these inflammatory factors across different types of immune cells.

With regard to interleukin signalings, we found that the levels of interleukin 1B (*IL1B*) and *IL15* in monocytes and cDC2 were significantly elevated in patients compared to the control group (Fig. 4A–C). Whereas *IL16* expression in lymphoid cells was significantly decreased in patients [20], similar results were showed about *IL32* and *IL18* in T and cDC2 cells, respectively (Fig. 4D, **Supplementary Fig. 1A,B**). Regarding interleukin receptors, we found that *IL2RG* and *IL6ST* in lymphoid cells were significantly higher in patients with pMN (Fig. 4E). The similar trends were observed in monocytes and cDC2 for *IL6R* and *IL10RB*. Multiple scoring metrics further confirmed the findings (Fig. 4F).

In terms of interferon signaling, expression levels of interferon gamma (IFNG), IFNG antisense RNA1 (*IFNG-ASI*) and interferon alpha and beta receptor subunit 2 (*IF-NAR2*) in specific type cells were significantly higher in patients (Fig. 4G–I, **Supplementary Fig. 1C–F**).

Regarding the tumor necrosis factor superfamily, we noted that *TNFRSF13C*, *TNFAIP3*, *TNFAIP8* and *TNFSF8* in T cells were significantly upregulated in patients, as confirmed by specific score systems (Fig. 4J–N, **Supplementary Fig. 1G,I**). In contrast, expression levels of *TN-FSF13B* and *TNFRSF14* in lymphoid cells were downregulated in patients (Fig. 4J,L,M, **Supplementary Fig. 1H**).

Additionally, several chemokines in monocytes were higher in patients compared to healthy donors, including *CCL3L1*, *CXCL8* (*IL8*) and *CXCL10* (Fig. 4O–R, **Supplementary Fig. 1J**), with a similar trend for *CXCR4* in lym-



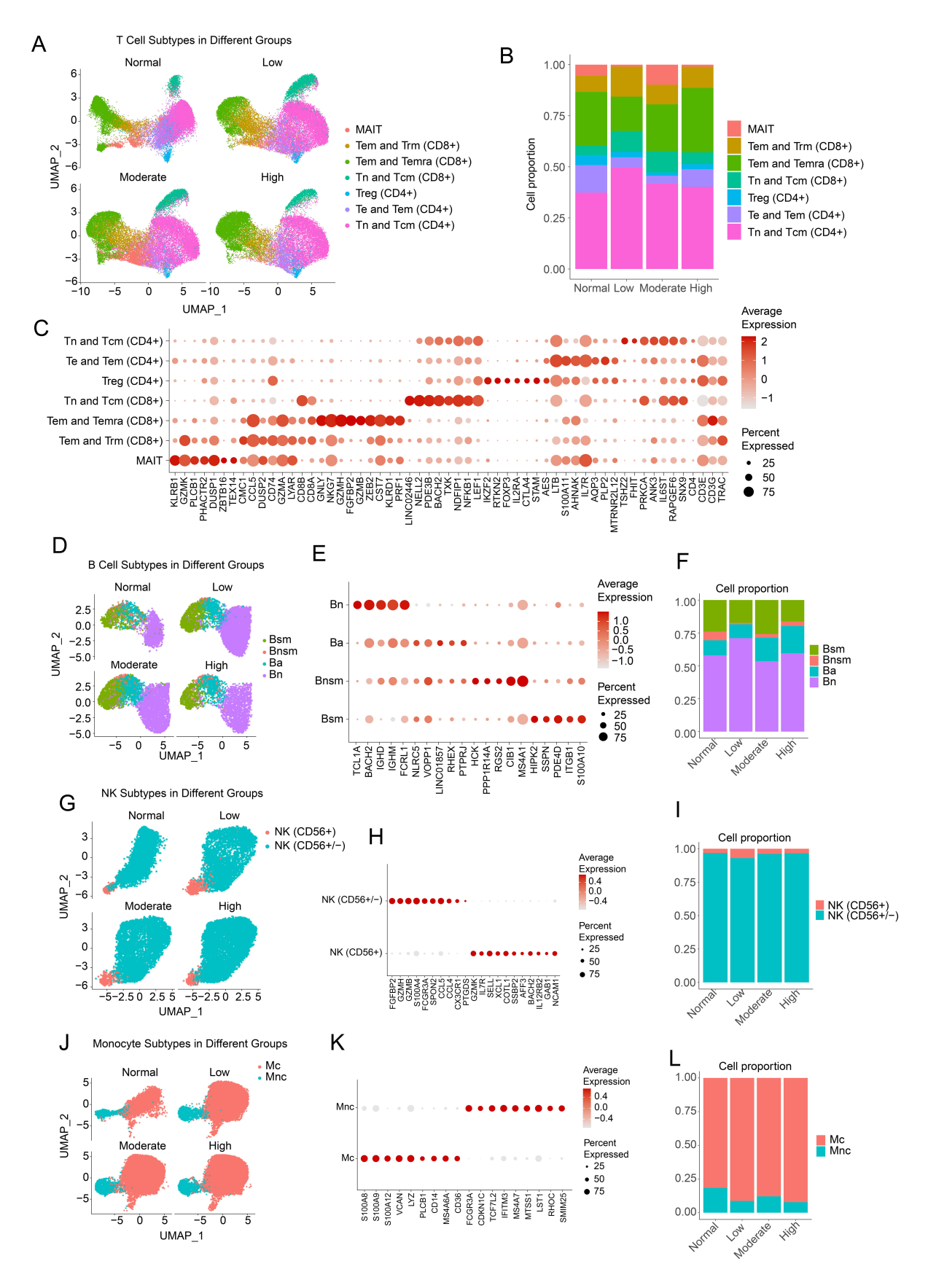


Fig. 2. Independent clusters and annotations of immune cell types. (A,D,G,J) UMAP visualized subtypes of T, B, NK cells and monocytes, respectively. (C,E,H,K) Dot plots showing expression of marker genes in each subclusters. (B,F,I,L) Bar plots of the proportion of cell subtypes among the four groups (normal, low-risk, moderate-risk and high-risk).

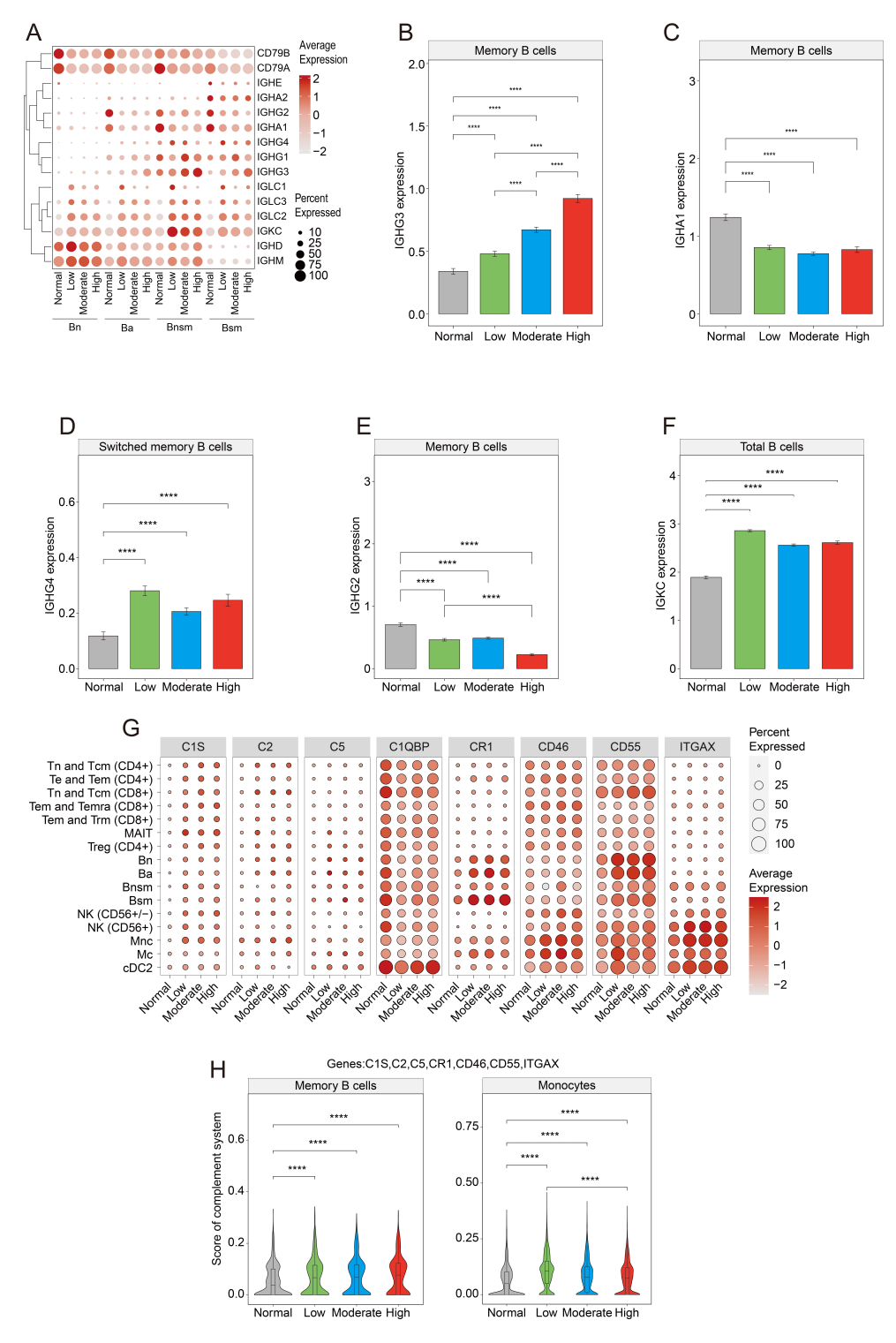


Fig. 3. Gene expression of immunoglobulins and complement system across different groups. (A) Dot plot showing genes of immunoglobulin heavy and light chains and B cell receptors in naive and activated B cells, non-switched and switched memory B cells. (B,D,F) Expression of genes IGHG3, IGHG4 and IGKC were higher in patients than in healthy donors. Lines indicate means \pm SEM. (C,E) Expression of genes IGHA1 and IGHG2 were lower in patients. (G) Dot plot showing genes of complement system in T, B, NK, monocytes and cDC2. (H) Score of complement system included genes CIS, C2, C5, CR1, CD46, CD55 and ITGAX. Individual violin plots containing a box plot, showing the median expression value of the score. ****, p < 0.0001. IGHG3, immunoglobulin heavy constant gamma 3; IGKC, immunoglobulin kappa constant; IGHA1, immunoglobulin heavy constant alpha 1; C1S, complement C1s.

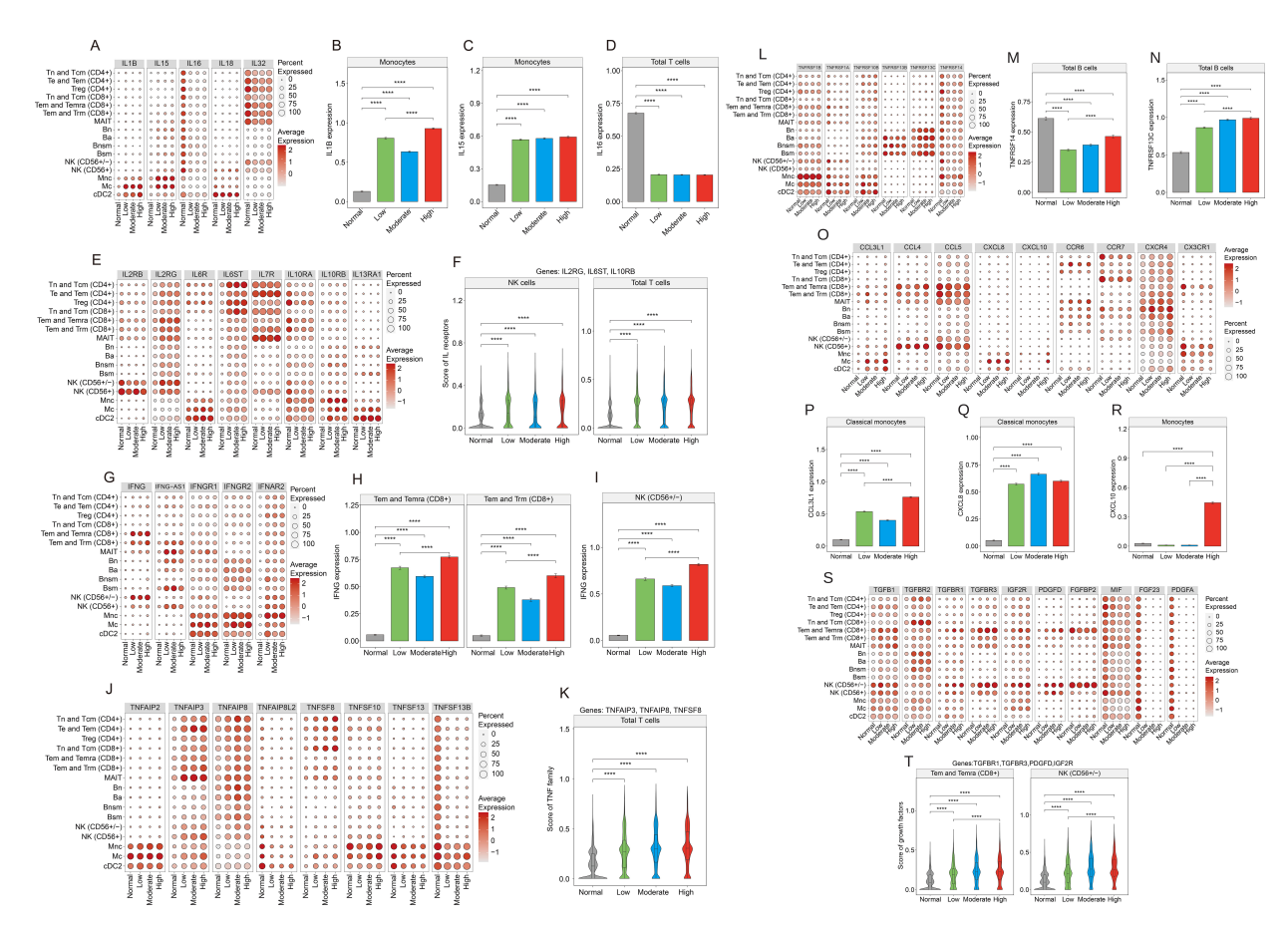


Fig. 4. Expression of proinflammatory factors and chemokines related genes across different groups. (A) Dot plot showing expression of interleukins in specific type cells. (B–D) Average expression of IL1B, IL15 and IL16 in monocytes and T cells, respectively. (E) Dot plot showing expression of interleukin receptors in individual type cells. (F) Scores of interleukin receptors included genes IL2RG, IL6ST and IL10RB. Individual violin plots containing a box plot, showing the median expression value of the score. (G) Dot plot showing expression of interferons and their receptors in different type cells. (H,I) Average expression of IFNG in Tem and Temra (CD8⁺) and NK (CD56^{+/-}) cells. (J) Dot plot showing expression of some tumor necrosis factors in individual type cells. (K) Violin plot showing score of TNF family members including TFAIP3, TNFAIP8 and TNFSF18 in total T cells. (L) Dot plot showing expression of TNF receptors in four different groups. (M,N) The average expression of TNFRSF14 and TNFR13C in total B cells. (O) Dot plot showing expression of chemokines and their receptors in individual type cells. (P–R) Average expression of chemokines such as CCL3L1, CXCL8 and CXCL10 in classical monocytes and total monocytes. (S) Dot plot showing expression of growth factors and their receptors in different type cells. (T) Violin plots showing score of growth factors including TGFBR1, TGFBR3, PDGFD and TGF2R in Tem, Temra (CD8⁺) and NK (CD56^{+/-}) cells, respectively. ****, p < 0.0001. IFNG, interferon G; interleukin 2 receptor subunit gamma; IL6ST, interleukin 6 cytokine family signal transducer; IL10RB, interleukin 10 receptor subunit beta; TNF, tumor necrosis factor; CCL3L1, C-C motif chemokine ligand 3 like 1; CXCL8, C-X-C motif chemokine ligand 8; TGFBR1, transforming growth factor beta receptor 1; PDGFD, platelet derived growth factor D; IGF2R, insulin like growth factor 2 receptor.

phoid cells (**Supplementary Fig. 1K**). In contrast, expression levels of *CX3CR1* and *CCR7* in specific kinds of cells were relatively lower in patients.

Growth factors also play an essential role in inflammatory responses. Scores of growth-factor family members (*TGFBR1*, *TGFBR3*, *IGF2R* and *PDGFD*) were significantly higher in patients with pMN, with a similar trend in high-risk patients compared to low-risk group (Fig. 4S,T). Conversely, expression levels of some factors (*MIF*, *FGF23* and *PDGFA*) significantly decreased in patients than in the control group.

Taken together, these data indicate that a range of proinflammatory pathways is activated, contributing to the development of pMN with anti-PLA2R1 antibodies.

3.4 Pattern Recognition Receptor Signaling Participating in The Development of pMN

It is well established that proinflammatory responses are often activated by pattern recognition receptors (PRRs) signalings [21], which includes toll-like receptors (TLRs) [22], NOD-like receptors (NLRs) [23], RNA sensors (RIG-I like receptors, RLRs) [24], DNA sensors (cyclic GMP-



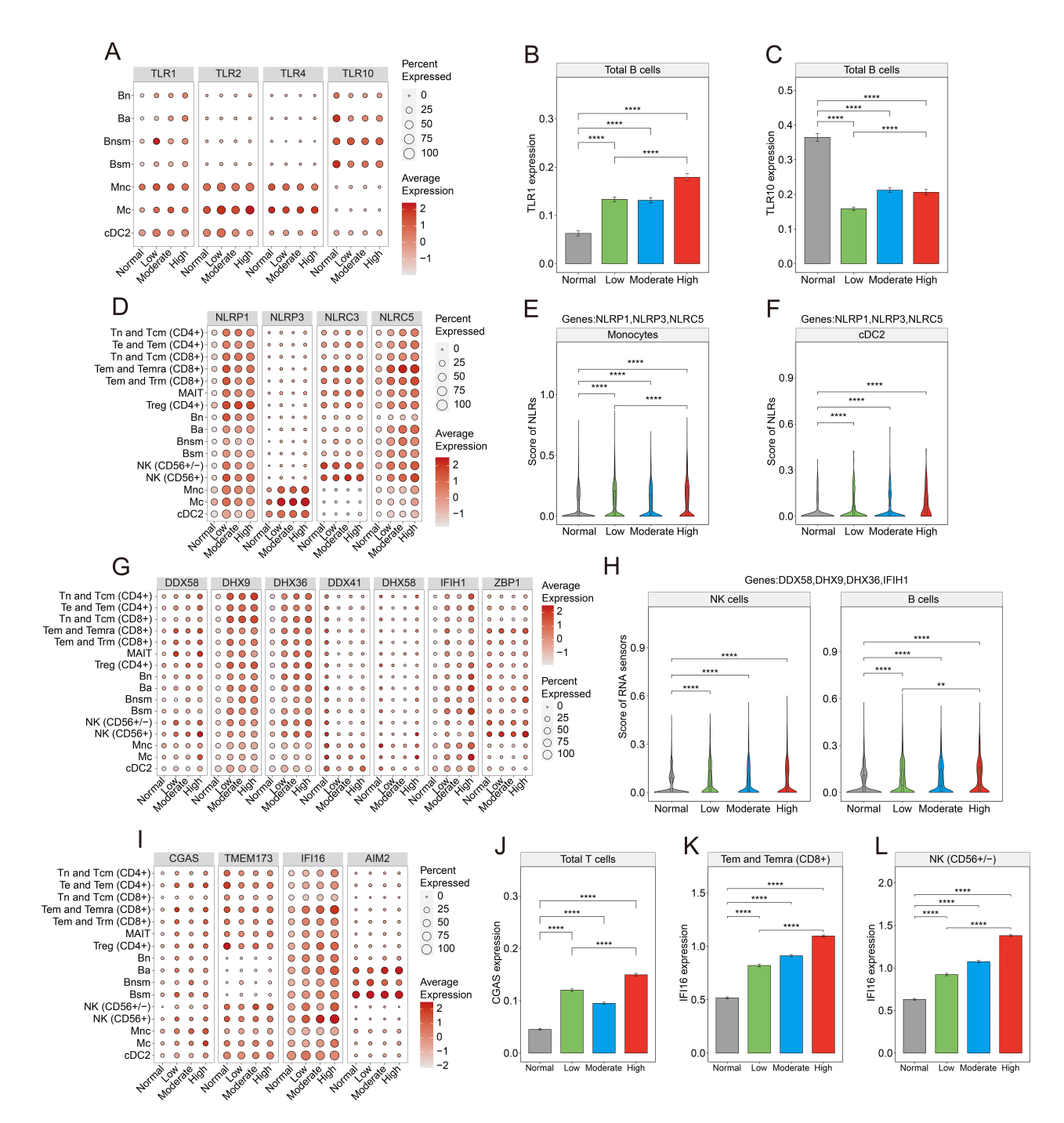


Fig. 5. Pattern recognition receptors involved into the development of pMN. (A) Dot plot showing expression of Toll-like receptors in B cells, monocytes and cDC2. (B,C) Average expression of TLR1 and TLR10 in total B cells. (D) Dot plot showing expression of NOD-like receptors in individual type cells. (E,F) Violin plot showing score of NLRs in monocytes and cDC2, consisting of NLRP1, NLRP3 and NLRC5. (G) Dot plot showing expression of RNA sensors in different type of cells. (H) Violin plot showing score of RNA sensors including DDX58, DHX9, DHX36 and IFIH1 in total B and NK cells. (I) Dot plot showing expression of DNA sensors in different cells. (J–L) Average expression of cGAS and cGAS and

AMP synthase (cGAS) receptors, cGLRs) and so on [25]. To investigate whether PRR pathways participate into the development of pMN, we examined their expression in patients compared to healthy donors. Notably, many of the

PRRs in specific type of cells were elevated in patients, including *NLRs* (*NLRP1*, *NLRP3* and *NLRC5*) (Fig. 5D–F), RNA sensors (*DDX58*, *IFIH1*, *DDX9* and *DDX36*) (Fig. 5G,H), DNA sensors (*cGAS* and *IFI16*) (Fig. 5I–L)



and *TLR1* (Fig. 5A,B). In contrast, some were relatively lower in patients, such as *TLR10* (Fig. 5A,C) and *TMEM173* (Supplementary Fig. 1L).

Given the downstream effects of PRR signalings, we next examined the activation of transcript factors (TFs)-related pathways that are often implicated in immune response pathways. Interestingly, we found that several TF-related pathways were upregulated in patients than in healthy donors, including MAPKs, AP1 (FOS, JUN, JUNB and JUND), janus kinase (JAK) and signal transducer and activator of transcription (STAT) members (JAK1, JAK2 and STAT3), nuclear factor kappa B family (NFKB1, RELB and NFKB1A), forkhead domain family (FOXO1 and FOXO3), TRAF3, HIF1A and IRF1 (Supplementary Fig. 2) [26–28].

Together, these results suggest that a broad range of innate immune signaling pathways in PBMCs may play a role in the pathogenesis of pMN with anti-PLA2R1 antibodies.

3.5 Biological Processes Mediated Dysfunction of Immune Cells in pMN

According to the data of different expression genes (DEGs) between patients and healthy donors, we found several interesting biological processes enriched in patients, which might affect the function of immune cells. Cellular senescence plays a key role in chronic diseases, including autoimmune diseases, metabolic diseases and tumors [29]. We found that a senescence-related gene panel was significantly enriched in patients than in the control group (Supplementary Fig. 3A). Statistically, integrated score of cellular senescent genes was higher in immune cells of patients (Supplementary Fig. 3B-D). In terms of circadian rhythm and chromatin remodeling, similar trends were showed in patients (Supplementary Fig. 3E-K) [30–32]. Altogether, these functional abnormalities of immune cells in pMN need to be explored comprehensively, which would offer more potential therapy targets for patients with pMN.

3.6 Antiviral Defense Response Associated with The Development of High-risk pMN

Although there are some biomarkers used for distinguishing high-risk patients from others, such as proteinuria, serum albumin and eGFR [10], it is limited that our understanding of the immune pathogenesis in the development of high-risk pMN. To address this issue, we analyzed the DEGs between high-risk and low-risk patients.

Intriguingly, genes of defense response to viruses in T, NK cells and monocytes were significantly upregulated in the high-risk group compared to the low-risk group (Fig. 6A,B,G,H,J,K) [33,34]. Similarly, interferonmediated signaling pathway in B cells was more active in high-risk group (Fig. 6D,E). In cDC2 cells, genes related to antigen presentation were significantly increased in high-risk patients (Fig. 6M,N), as confirmed by scores of upregulated gene sets (Fig. 6C,F,I,L,O). Of note, all of the

scores were also effective for distinguishing high-risk patients from moderate-risk population.

In order to develop a score system for identifying high-risk patients in the overall population, we selected upregulated genes in high-risk patients compared to low-risk individuals in most types of immune cells, including *SLC35F1*, *AC105402.3*, *STAT1*, *EPSTI1*, *MX1* and *EIF2AK2* (**Supplementary Fig. 4A,B**). The gene *TRIM22* was excluded due to its high expression in healthy donors (**Supplementary Fig. 4A**). Importantly, this score system was also effective in distinguishing high-risk patients from moderate-risk individuals.

To further distinguishing moderate-risk patients from high-risk and low-risk populations, we selected genes gradually upregulated from low-risk to high-risk patients in most types of immune cells to develop different score systems (**Supplementary Fig. 4C,E–G**). Notably, *SLC35F1* in B cells was a valuable biomarker for distinguishing the three risk groups (**Supplementary Fig. 4D**) [35,36].

3.7 The Predictable Effect of Biomarkers for Identifying High-Risk Patients with pMN

To confirm the predictable value of upregulated biomarkers in high-risk patients compared to low-risk population, we performed correlation analysis between these biomarkers and eGFR in newly-diagnosed patients with pMN. As shown in Table 2 and **Supplementary Fig. 5**, most effective biomarkers were negatively correlated with eGFR. Of note, upregulation of *SLC35F1* and *BTS2* in most types of PBMCs could effectively predict poor kidney function. Both *GBP5* and *KLF6* also had the predictable role in more than one type of immune cells. Conversely, only two genes (*LRMDA* and *MYO1F*) were positively associated with eGFR in cDC2 cells.

Given the small sample size of our study, we attempted to figure out whether the screened biomarkers enriched in high-risk patients had a robust capability of predicting declined eGFR in the development of nephrotic syndrome and other chronic kidney diseases (Nephroseq v5 database). Indeed, the predictable values of most biomarkers were confirmed in a larger population (Supplementary Table 2). Despite the validated results were calculated based on kidney tissues, this fact suggests that biomarkers in blood cells have a similar effect on risk stratification.

In addition, we assessed the predictable values of prior selected biomarkers upregulated in total patients with pMN compared to healthy donors. Similarly, most of them were negatively correlated with declined eGFR in patients with nephrotic syndrome or other chronic kidney diseases (Supplementary Table 3).

Altogether, we identified a series of effective biomarkers used for distinguishing high-risk patients from low-risk individuals with pMN and for predicting declined eGFR of patients.



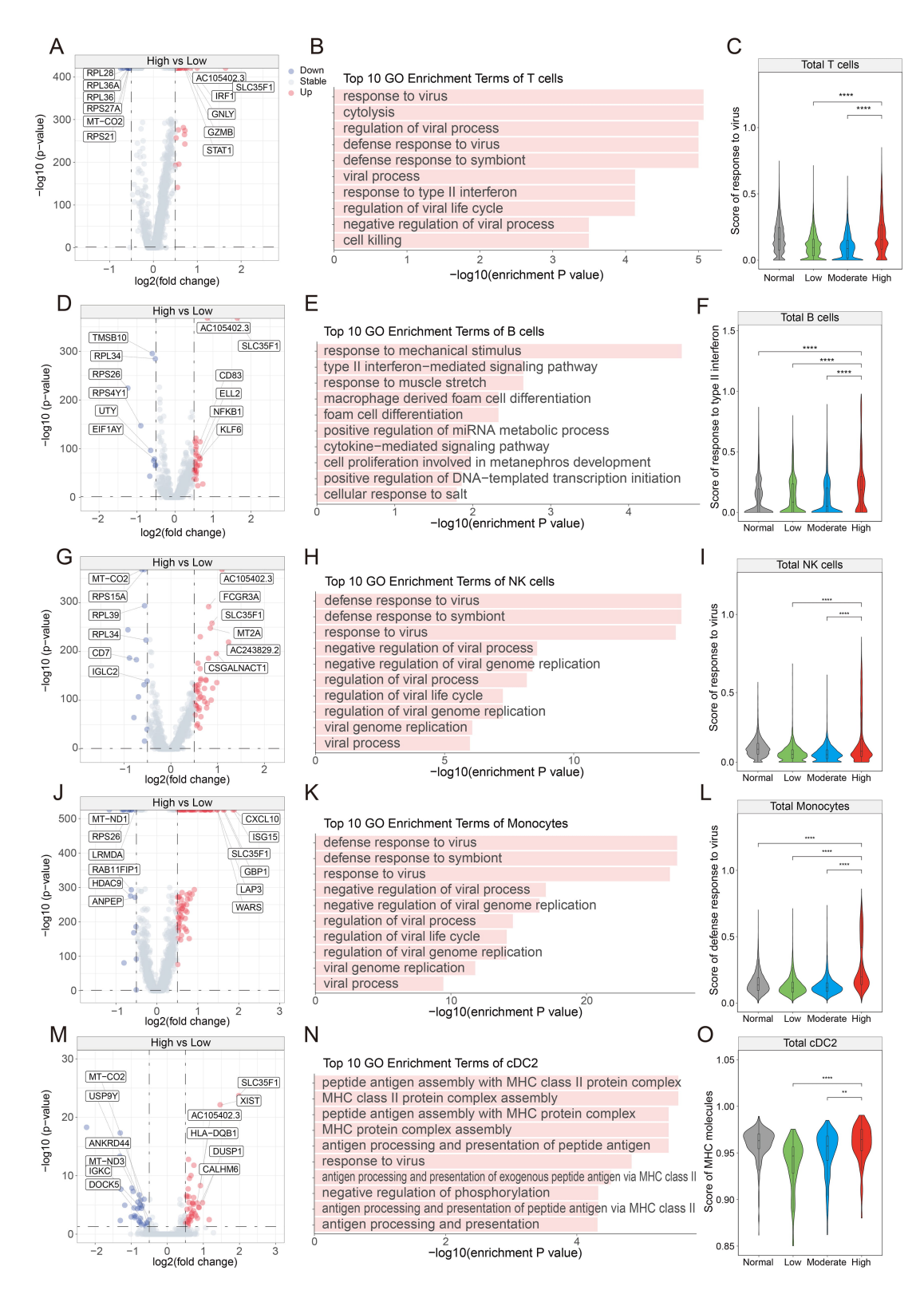


Fig. 6. The top 10 upregulated GO enrichment terms in immune cells from high-risk patients compared with low-risk individuals with pMN. (A,D,G,J,M) Volcano plots showing log2 fold change in gene expression in T, B, NK, monocytes and cDC2 from high-risk patients, respectively. (B,E,H,K,N) The top upregulated 10 Go enrichment terms of T, B, NK, monocytes and cDC2 from high-risk patients, respectively. (C,F,I,L,O) Violin plots showing increased scores of response to virus in T, NK cells and monocytes from high-risk patients, respectively; score of response to type II interferon-mediated signaling in B cells from high-risk patients; score of antigen presentation molecules in cDC2 from high-risk patients. **, p < 0.01; ****, p < 0.0001.

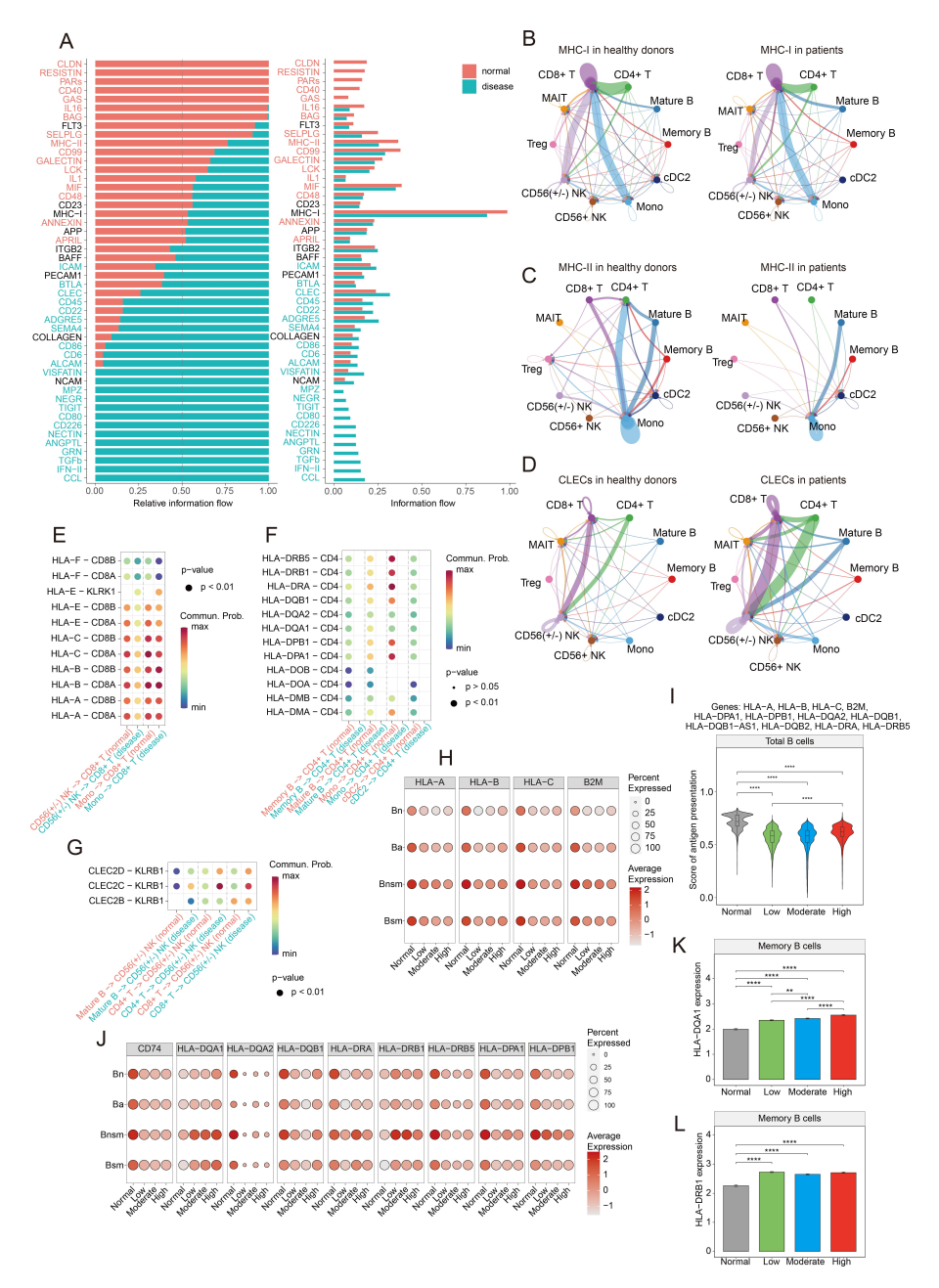


Fig. 7. Differential cell-to-cell communications between patients with pMN and healthy control. (A) Relative and absolute flows of differentially active signaling pathways between patients with pMN and healthy donors (two-sided Wilcoxon test; FDR >0.05). blue bars represented relative enrichment signalings in pMN, red bars indicated enriched pathways in healthy donors. (B–D) Chord plots showing changes of *MHC-I*, *MHC-II* and *CLEC* signaling pathways in patients and healthy donors. The width of a band indicated the predicted strength of a specific ligand-receptor pair interactions. The wider the band, the stronger relationship between the pairs. (E) Comparison of the significant ligand-receptor pairs from NK (CD56+/-) or monocytes with HLA-I to T (CD8+) cells between patients and healthy control. Dot color reflecting communication probabilities and dot size representing computed *p*-values. (F) Comparison of the significant ligand-receptor pairs from B cells, monocytes or cDC2 with HLA-II to T (CD4+) cells between patients and healthy donors. (G) Comparison of the significant ligand-receptor pairs from mature B or T cells with CLECs to NK (CD56+/-) cells between patients and healthy donors. (H,J) Dot plot showing expression levels of *HLA-I* and molecules in all of B subsets across four groups, respectively. (I) Violin plot showing score of *HLA-I* and *HLA-II* in total B cells. (K,L) Average expression of *HLA-DQA1* and *HLA-DRB1* in memory B cells across four groups. **, p < 0.001; ****, p < 0.0001. MHC-I, major histocompatibility complex, class I; HLA-I, human leukocyte antigen, class II, DR beta 1; HLA-DQA1, human leukocyte antigen, class II, DR beta 1; HLA-DQA1, human leukocyte antigen, class II, DR alpha 1; CLEC2B, C-type lectin domain family 2 member B; CLEC2C, C-type lectin domain family 2 member C; CLEC2D, C-type lectin domain family 2 member D; KLRB1, killer cell lectin like receptor B1.

Table 2. Biomarkers identified in high-risk patients predict declined eGFR.

Gene Disease Cell type Samples (n) Outcome R p B2M pMN cDC2 10 eGFR -0.77 *** BST2 pMN T 10 eGFR -0.83 *** BST2 pMN NK 10 eGFR -0.90 **** LA Mon 10 eGFR -0.89 **** DUSP1 pMN B 10 eGFR -0.70 * DUSP1 pMN B 10 eGFR -0.77 *** ELL2 pMN B 10 eGFR -0.66 * FGL2 pMN Mon 10 eGFR -0.65 * FKBP5 pMN NK 10 eGFR -0.72 * FKBP5 pMN T 10 eGFR -0.70 * HSP90AA1 pMN Mon 10 eGFR -0.72 * KLF6							
BST2	Gene	Disease	Cell type	Samples (n)	Outcome	R	p
NK 10 eGFR -0.90 *** Mon 10 eGFR -0.90 *** DNAJB4 pMN B 10 eGFR -0.70 * DUSP1 pMN cDC2 10 eGFR -0.77 ** ELL2 pMN B 10 eGFR -0.66 * FGL2 pMN Mon 10 eGFR -0.65 * FKBP5 pMN NK 10 eGFR -0.73 * RFKBP5 pMN Mon 10 eGFR -0.73 * HSP90AA1 pMN Mon 10 eGFR -0.70 * NK 10 eGFR -0.70 * NK 10 eGFR -0.69 * RFT pMN Mon 10 eGFR -0.69 * RFT pMN Mon 10 eGFR -0.69 * RAMTOR2 pMN cDC2 10 eGFR -0.76 ** LAMTOR2 pMN cDC2 10 eGFR -0.65 * MYO1F pMN cDC2 10 eGFR -0.65 * NK 10 eGFR -0.70 ** B 10 eGFR -0.69 * LAMTOR1 pMN CDC2 10 eGFR -0.70 ** MTSS1 pMN NK 10 eGFR -0.65 * MYO1F pMN cDC2 10 eGFR -0.65 * MYO1F pMN cDC2 10 eGFR -0.66 ** PDCD2 pMN cDC2 10 eGFR -0.66 ** NFKBIA pMN B 10 eGFR -0.64 * PDCD2 pMN cDC2 10 eGFR -0.67 *** PSMA4 pMN Mon 10 eGFR -0.87 *** PSMB9 pMN Mon 10 eGFR -0.87 *** PSMB9 pMN Mon 10 eGFR -0.86 ** SAT1 pMN Mon 10 eGFR -0.86 ** SAT1 pMN Mon 10 eGFR -0.86 ** SLC27A4 pMN cDC2 10 eGFR -0.81 ** NK 10 eGFR -0.80 ** SLC35F1 pMN NK 10 eGFR -0.81 ** NK 10 eGFR -0.77 ** SLFN5 pMN NK 10 eGFR -0.80 ** TNFAIP3 pMN Mon 10 eGFR -0.77 ** SLFN5 pMN NK 10 eGFR -0.77 **	B2M	pMN	cDC2	10	eGFR	-0.77	**
Mon 10 eGFR -0.89 ***	BST2	pMN	T	10	eGFR	-0.83	**
DNAJB4 pMN B 10 eGFR -0.91 ** DNAJB4 pMN B 10 eGFR -0.70 * DUSP1 pMN cDC2 10 eGFR -0.77 ** ELL2 pMN B 10 eGFR -0.66 * FGL2 pMN Mon 10 eGFR -0.65 * FKBP5 pMN NK 10 eGFR -0.72 * NK 10 eGFR -0.70 * HSP90AA1 pMN Mon 10 eGFR -0.70 * HSP90AA1 pMN Mon 10 eGFR -0.69 * IRF1 pMN Mon 10 eGFR -0.69 * IRF1 pMN Mon 10 eGFR -0.69 * LAMTOR2 pMN cDC2 10 eGFR -0.76 ** LAMTOR2 pMN cDC2 10 eGFR -0.65 * MYO1F pMN CDC2 10 eGFR -0.66 ** PDCD2 pMN cDC2 10 eGFR -0.67 ** PSMA4 pMN Mon 10 eGFR -0.64 * PDCD2 pMN cDC2 10 eGFR -0.87 *** PSMB9 pMN Mon 10 eGFR -0.87 *** PSMB9 pMN Mon 10 eGFR -0.87 *** SAT1 pMN Mon 10 eGFR -0.86 ** SAT1 pMN Mon 10 eGFR -0.81 ** SFRS7 pMN cDC2 10 eGFR -0.86 ** SLC27A4 pMN cDC2 10 eGFR -0.80 ** SLC35F1 pMN T 10 eGFR -0.81 ** NK 10 eGFR -0.81 ** NK 10 eGFR -0.77 ** SLFN5 pMN NK 10 eGFR -0.77 **			NK	10	eGFR	-0.90	***
DNAJB4 pMN B 10 eGFR -0.70 * DUSP1 pMN cDC2 10 eGFR -0.66 * ELL2 pMN B 10 eGFR -0.66 * FGL2 pMN Mon 10 eGFR -0.65 * FKBP5 pMN NK 10 eGFR -0.73 * GBP5 pMN T 10 eGFR -0.72 * HSP90AA1 pMN Mon 10 eGFR -0.69 * HSP90AA1 pMN Mon 10 eGFR -0.69 * IRF1 pMN Mon 10 eGFR -0.69 * KLF6 pMN T 10 eGFR -0.72 * LAMTOR2 pMN cDC2 10 eGFR -0.76 ** LAMTOR2 pMN cDC2 10 eGFR -0.65 * MYO1F<			Mon	10	eGFR	-0.89	***
DUSP1 pMN cDC2 10 eGFR -0.77 ** ELL2 pMN B 10 eGFR -0.66 * FGL2 pMN Mon 10 eGFR -0.65 * FKBP5 pMN NK 10 eGFR -0.73 * GBP5 pMN T 10 eGFR -0.72 * HSP90AA1 pMN Mon 10 eGFR -0.69 * HSP90AA1 pMN Mon 10 eGFR -0.69 * HSP90AA1 pMN Mon 10 eGFR -0.69 * IRF1 pMN Mon 10 eGFR -0.69 * KLF6 pMN T 10 eGFR -0.72 * LAMTOR2 pMN cDC2 10 eGFR -0.76 ** LAMTOR2 pMN cDC2 10 eGFR -0.65 * M			cDC2	10	eGFR	-0.91	**
ELL2 pMN B 10 eGFR -0.66 * FGL2 pMN Mon 10 eGFR -0.65 * FKBP5 pMN NK 10 eGFR -0.73 * GBP5 pMN T 10 eGFR -0.72 * NK 10 eGFR -0.69 * IRF1 pMN Mon 10 eGFR -0.82 ** KLF6 pMN T 10 eGFR -0.72 * B 10 eGFR -0.72 * B 10 eGFR -0.69 * IRF1 pMN Mon 10 eGFR -0.69 * IRF1 pMN CDC2 10 eGFR -0.76 ** IRMDA pMN cDC2 10 eGFR -0.76 ** MYO1F pMN cDC2 10 eGFR -0.65 * MYO1F pMN cDC2 10 eGFR -0.65 * MYO1F pMN B 10 eGFR -0.65 * NFKBIA pMN B 10 eGFR -0.64 * PDCD2 pMN CDC2 10 eGFR -0.77 ** PSMB9 pMN Mon 10 eGFR -0.87 *** PSMB9 pMN Mon 10 eGFR -0.87 *** PSME2 pMN Mon 10 eGFR -0.86 ** SAT1 pMN Mon 10 eGFR -0.86 ** SAT1 pMN Mon 10 eGFR -0.86 ** SLC27A4 pMN cDC2 10 eGFR -0.86 ** SLC27A4 pMN CDC2 10 eGFR -0.86 ** SLC35F1 pMN T 10 eGFR -0.86 ** SLC35F1 pMN T 10 eGFR -0.86 ** SLFN5 pMN NK 10 eGFR -0.77 ** SLFN5 pMN NK 10 eGFR -0.80 ** TNFAIP3 pMN Mon 10 eGFR -0.77 ** SLFN5 pMN Mon 10 eGFR -0.80 ** TNFAIP3 pMN Mon 10 eGFR -0.79 ** TSC22D3 pMN CDC2 10 eGFR -0.71 * TYMP pMN Mon 10 eGFR -0.71 *	DNAJB4	pMN	В	10	eGFR	-0.70	*
FGL2 pMN Mon 10 eGFR -0.65 * FKBP5 pMN NK 10 eGFR -0.73 * GBP5 pMN T 10 eGFR -0.72 * HSP90AA1 pMN Mon 10 eGFR -0.69 * HSP90AA1 pMN Mon 10 eGFR -0.69 * IRF1 pMN Mon 10 eGFR -0.69 * KLF6 pMN T 10 eGFR -0.72 * LAMTOR2 pMN cDC2 10 eGFR -0.69 * LAMTOR2 pMN cDC2 10 eGFR -0.69 * LAMTOR2 pMN cDC2 10 eGFR -0.76 ** LAMTOR2 pMN cDC2 10 eGFR -0.69 * LAMTOR2 pMN cDC2 10 eGFR -0.67 **	DUSP1	pMN	cDC2	10	eGFR	-0.77	**
FKBP5 pMN NK 10 eGFR -0.73 * GBP5 pMN T 10 eGFR -0.72 * NK 10 eGFR -0.70 * HSP90AA1 pMN Mon 10 eGFR -0.69 * IRF1 pMN Mon 10 eGFR -0.82 ** KLF6 pMN T 10 eGFR -0.69 * IRF1 pMN CDC2 10 eGFR -0.69 * LAMTOR2 pMN cDC2 10 eGFR -0.65 * LAMTOR3 pMN NK 10 eGFR -0.65 * MYO1F pMN cDC2 10 eGFR -0.65 * MYO1F pMN cDC2 10 eGFR -0.64 * PDCD2 pMN cDC2 10 eGFR -0.64 * PDCD2 pMN DOC2 10 eGFR -0.64 * PSMA4 pMN B 10 eGFR -0.64 * PSMB9 pMN Mon 10 eGFR -0.87 *** PSMB9 pMN Mon 10 eGFR -0.87 *** PSME2 pMN Mon 10 eGFR -0.86 ** SAT1 pMN Mon 10 eGFR -0.86 ** SAT1 pMN Mon 10 eGFR -0.86 ** SAT1 pMN CDC2 10 eGFR -0.86 ** SAT1 pMN Mon 10 eGFR -0.86 ** SAT1 pMN Mon 10 eGFR -0.86 ** SLC27A4 pMN cDC2 10 eGFR -0.80 ** B 10 eGFR -0.70 * SLC35F1 pMN T 10 eGFR -0.81 ** Mon 10 eGFR -0.77 ** SLFN5 pMN NK 10 eGFR -0.77 ** SLFN5 pMN MON 10 eGFR -0.79 ** TYMP pMN MON 10 eGFR -0.79 **	ELL2	pMN	В	10	eGFR	-0.66	*
GBP5 pMN T 10 eGFR -0.72 * NK 10 eGFR -0.70 * HSP90AA1 pMN Mon 10 eGFR -0.69 * IRF1 pMN Mon 10 eGFR -0.82 ** KLF6 pMN T 10 eGFR -0.69 * LAMTOR2 pMN cDC2 10 eGFR -0.69 * LRMDA pMN cDC2 10 eGFR 0.79 ** MTSS1 pMN NK 10 eGFR -0.65 * MY01F pMN cDC2 10 eGFR -0.65 * MY01F pMN cDC2 10 eGFR -0.64 * PDCD2 pMN cDC2 10 eGFR -0.87 *** PSMA4 pMN B 10 eGFR -0.87 *** PSMB9 pMN Mon 10 eGFR -0.87 *** PSME2 pMN Mon 10 eGFR -0.86 ** SAT1 pMN Mon 10 eGFR -0.86 ** SAT1 pMN Mon 10 eGFR -0.86 ** SLC27A4 pMN cDC2 10 eGFR -0.86 ** SLC27A4 pMN cDC2 10 eGFR -0.86 ** SLC35F1 pMN T 10 eGFR -0.80 ** B 10 eGFR -0.81 ** NK 10 eGFR -0.81 ** NK 10 eGFR -0.77 ** SLFN5 pMN NK 10 eGFR -0.77 ** SLFN5 pMN NK 10 eGFR -0.77 ** SLFN5 pMN NK 10 eGFR -0.79 ** TNFAIP3 pMN Mon 10 eGFR -0.79 ** TNFAIP3 pMN Mon 10 eGFR -0.79 ** TYMP pMN Mon 10 eGFR -0.71 *	FGL2	pMN	Mon	10	eGFR	-0.65	*
NK 10 eGFR -0.70 * HSP90AA1 pMN Mon 10 eGFR -0.69 * IRF1 pMN Mon 10 eGFR -0.82 ** KLF6 pMN T 10 eGFR -0.72 * B 10 eGFR -0.69 * LAMTOR2 pMN cDC2 10 eGFR -0.76 ** LRMDA pMN cDC2 10 eGFR 0.79 ** MTSS1 pMN NK 10 eGFR -0.65 * MYO1F pMN cDC2 10 eGFR -0.65 * MYO1F pMN cDC2 10 eGFR -0.64 * PDCD2 pMN cDC2 10 eGFR -0.87 *** PSMA4 pMN B 10 eGFR -0.87 *** PSMB9 pMN Mon 10 eGFR -0.87 ** PSME2 pMN Mon 10 eGFR -0.86 ** SAT1 pMN Mon 10 eGFR -0.71 * SFRS7 pMN cDC2 10 eGFR -0.86 ** SLC27A4 pMN cDC2 10 eGFR -0.86 ** SLC27A4 pMN CDC2 10 eGFR -0.86 ** SLC35F1 pMN T 10 eGFR -0.80 ** B 10 eGFR -0.81 ** NK 10 eGFR -0.81 ** NK 10 eGFR -0.77 ** SLFN5 pMN NK 10 eGFR -0.77 ** SLFN5 pMN NK 10 eGFR -0.77 ** SLFN5 pMN NK 10 eGFR -0.79 ** TNFAIP3 pMN Mon 10 eGFR -0.79 ** TNFAIP3 pMN Mon 10 eGFR -0.71 * TYMP pMN Mon 10 eGFR -0.71 *	FKBP5	pMN	NK	10	eGFR	-0.73	*
HSP90AA1 pMN Mon 10 eGFR -0.69 * IRF1 pMN Mon 10 eGFR -0.82 ** KLF6 pMN T 10 eGFR -0.72 * B 10 eGFR -0.69 * LAMTOR2 pMN cDC2 10 eGFR -0.76 ** LRMDA pMN cDC2 10 eGFR -0.65 * MYO1F pMN cDC2 10 eGFR -0.65 * MYO1F pMN cDC2 10 eGFR -0.65 * MYO1F pMN cDC2 10 eGFR -0.64 * PDCD2 pMN cDC2 10 eGFR -0.87 *** PSMA4 pMN B 10 eGFR -0.87 *** PSMB9 pMN Mon 10 eGFR -0.87 ** PSME2 pMN Mon 10 eGFR -0.86 ** SAT1 pMN Mon 10 eGFR -0.86 ** SAT1 pMN Mon 10 eGFR -0.86 ** SLC27A4 pMN cDC2 10 eGFR -0.86 ** SLC27A4 pMN cDC2 10 eGFR -0.86 ** SLC35F1 pMN T 10 eGFR -0.80 ** B 10 eGFR -0.81 ** Mon 10 eGFR -0.77 ** SLFN5 pMN NK 10 eGFR -0.77 ** SLFN5 pMN NK 10 eGFR -0.77 ** SLFN5 pMN NK 10 eGFR -0.79 ** TNFAIP3 pMN Mon 10 eGFR -0.79 ** TSC22D3 pMN cDC2 10 eGFR -0.79 ** TYMP pMN Mon 10 eGFR -0.71 *	GBP5	pMN	T	10	eGFR	-0.72	*
IRF1 pMN Mon 10 eGFR -0.82 ** KLF6 pMN T 10 eGFR -0.69 * LAMTOR2 pMN cDC2 10 eGFR -0.76 ** LRMDA pMN cDC2 10 eGFR -0.65 * MYO1F pMN cDC2 10 eGFR -0.65 * MYO1F pMN cDC2 10 eGFR -0.64 * PDCD2 pMN cDC2 10 eGFR -0.64 * PDCD2 pMN cDC2 10 eGFR -0.87 *** PSMA4 pMN B 10 eGFR -0.87 *** PSMB9 pMN Mon 10 eGFR -0.87 ** PSME2 pMN Mon 10 eGFR -0.86 ** SAT1 pMN Mon 10 eGFR -0.86 ** SAT1 pMN Mon 10 eGFR -0.86 ** SLC27A4 pMN cDC2 10 eGFR -0.86 ** SLC27A4 pMN cDC2 10 eGFR -0.86 ** SLC35F1 pMN T 10 eGFR -0.81 ** Mon 10 eGFR -0.80 ** SLC35F1 pMN K 10 eGFR -0.77 ** SLFN5 pMN NK 10 eGFR -0.79 ** TNFAIP3 pMN Mon 10 eGFR -0.79 ** TSC22D3 pMN cDC2 10 eGFR -0.71 *			NK	10	eGFR	-0.70	*
KLF6 pMN T 10 eGFR -0.72 * LAMTOR2 pMN cDC2 10 eGFR -0.69 * LAMTOR2 pMN cDC2 10 eGFR -0.76 ** LRMDA pMN cDC2 10 eGFR 0.79 ** MTSS1 pMN NK 10 eGFR -0.65 * MY01F pMN cDC2 10 eGFR 0.79 ** MY01F pMN cDC2 10 eGFR 0.65 * MY01F pMN B 10 eGFR -0.65 * MY01F pMN B 10 eGFR -0.64 * PDCD2 pMN B 10 eGFR -0.87 *** PSMA4 pMN Mon 10 eGFR -0.87 *** PSMB9 pMN Mon 10 eGFR -0.86 ** SAT	HSP90AA1	pMN	Mon	10	eGFR	-0.69	*
B 10 eGFR -0.69 * LAMTOR2 pMN cDC2 10 eGFR -0.76 ** LRMDA pMN cDC2 10 eGFR 0.79 ** MTSS1 pMN NK 10 eGFR -0.65 * MYO1F pMN cDC2 10 eGFR 0.79 ** NFKBIA pMN B 10 eGFR -0.64 * PDCD2 pMN cDC2 10 eGFR -0.87 *** PSMA4 pMN Mon 10 eGFR -0.87 ** PSMB9 pMN Mon 10 eGFR -0.86 ** SAT1 pMN Mon 10 eGFR -0.86 ** SAT1 pMN Mon 10 eGFR -0.86 ** SAT1 pMN CDC2 10 eGFR -0.86 ** SLC27A4 pMN cDC2 10 eGFR -0.86 ** SLC27A4 pMN cDC2 10 eGFR -0.86 ** SLC35F1 pMN T 10 eGFR -0.80 ** NK 10 eGFR -0.81 ** NK 10 eGFR -0.77 ** SLFN5 pMN NK 10 eGFR -0.77 ** SLFN5 pMN NK 10 eGFR -0.79 ** TNFAIP3 pMN Mon 10 eGFR -0.79 ** TSC22D3 pMN cDC2 10 eGFR -0.71 *	IRF1	pMN	Mon	10	eGFR	-0.82	**
LAMTOR2 pMN cDC2 10 eGFR -0.76 ** LRMDA pMN cDC2 10 eGFR 0.79 ** MTSS1 pMN NK 10 eGFR -0.65 * MYO1F pMN cDC2 10 eGFR 0.79 ** NFKBIA pMN B 10 eGFR -0.64 * PDCD2 pMN cDC2 10 eGFR -0.87 *** PSMA4 pMN Mon 10 eGFR -0.87 *** PSMB9 pMN Mon 10 eGFR -0.86 ** PSME2 pMN Mon 10 eGFR -0.86 ** SAT1 pMN Mon 10 eGFR -0.71 * SFRS7 pMN cDC2 10 eGFR -0.86 ** SLC27A4 pMN cDC2 10 eGFR -0.86 ** SLC35F1 pMN T 10 eGFR -0.80 ** B 10 eGFR -0.81 ** NK 10 eGFR -0.77 ** SLFN5 pMN NK 10 eGFR -0.77 ** SLFN5 pMN NK 10 eGFR -0.80 ** TNFAIP3 pMN Mon 10 eGFR -0.79 ** TSC22D3 pMN cDC2 10 eGFR -0.71 * TYMP pMN Mon 10 eGFR -0.71 *	KLF6	pMN	T	10	eGFR	-0.72	*
LRMDA pMN cDC2 10 eGFR 0.79 ** MTSS1 pMN NK 10 eGFR -0.65 * MYO1F pMN cDC2 10 eGFR 0.79 ** NFKBIA pMN B 10 eGFR -0.64 * PDCD2 pMN cDC2 10 eGFR -0.87 *** PSMA4 pMN Mon 10 eGFR -0.87 *** PSMB9 pMN Mon 10 eGFR -0.87 ** PSME2 pMN Mon 10 eGFR -0.86 ** SAT1 pMN Mon 10 eGFR -0.71 * SFRS7 pMN cDC2 10 eGFR -0.86 ** SLC27A4 pMN cDC2 10 eGFR -0.86 ** SLC35F1 pMN T 10 eGFR -0.80 ** B 10 eGFR -0.81 ** NK 10 eGFR -0.77 ** SLFN5 pMN NK 10 eGFR -0.77 ** SLFN5 pMN NK 10 eGFR -0.77 ** SLFN5 pMN NK 10 eGFR -0.77 ** TYMP pMN Mon 10 eGFR -0.71 *			В	10	eGFR	-0.69	*
MTSS1 pMN NK 10 eGFR -0.65 * MYO1F pMN cDC2 10 eGFR 0.79 ** NFKBIA pMN B 10 eGFR -0.64 * PDCD2 pMN cDC2 10 eGFR -0.87 *** PSMA4 pMN Mon 10 eGFR -0.87 *** PSMB9 pMN Mon 10 eGFR -0.87 ** PSME2 pMN Mon 10 eGFR -0.86 ** SAT1 pMN Mon 10 eGFR -0.71 * SFRS7 pMN cDC2 10 eGFR -0.86 ** SLC27A4 pMN cDC2 10 eGFR -0.86 ** SLC35F1 pMN T 10 eGFR -0.80 ** B 10 eGFR -0.81 ** NK 10 eGFR -0.77 ** Mon 10 eGFR -0.77 ** SLFN5 pMN NK 10 eGFR -0.77 ** SLFN5 pMN NK 10 eGFR -0.77 ** SLFN5 pMN NK 10 eGFR -0.77 ** TYMP pMN Mon 10 eGFR -0.71 *	LAMTOR2	pMN	cDC2	10	eGFR	-0.76	**
MYO1F pMN cDC2 10 eGFR 0.79 ** NFKBIA pMN B 10 eGFR -0.64 * PDCD2 pMN cDC2 10 eGFR -0.87 **** PSMA4 pMN Mon 10 eGFR -0.77 ** PSMB9 pMN Mon 10 eGFR -0.86 ** PSME2 pMN Mon 10 eGFR -0.86 ** SAT1 pMN Mon 10 eGFR -0.86 ** SLC27A4 pMN cDC2 10 eGFR -0.86 ** SLC35F1 pMN T 10 eGFR -0.80 ** B 10 eGFR -0.81 ** NK 10 eGFR -0.77 ** SLFN5 pMN NK 10 eGFR -0.80 ** TNFAIP3 pMN Mon 10 <	LRMDA	pMN	cDC2	10	eGFR	0.79	**
NFKBIA pMN B 10 eGFR -0.64 * PDCD2 pMN cDC2 10 eGFR -0.87 **** PSMA4 pMN Mon 10 eGFR -0.77 ** PSMB9 pMN Mon 10 eGFR -0.86 ** PSME2 pMN Mon 10 eGFR -0.86 ** SAT1 pMN Mon 10 eGFR -0.71 * SFRS7 pMN cDC2 10 eGFR -0.86 ** SLC27A4 pMN cDC2 10 eGFR -0.70 * SLC35F1 pMN T 10 eGFR -0.80 ** B 10 eGFR -0.81 ** NK 10 eGFR -0.77 ** SLFN5 pMN NK 10 eGFR -0.80 ** TNFAIP3 pMN Mon 10 <t< td=""><td>MTSS1</td><td>pMN</td><td>NK</td><td>10</td><td>eGFR</td><td>-0.65</td><td>*</td></t<>	MTSS1	pMN	NK	10	eGFR	-0.65	*
PDCD2 pMN cDC2 10 eGFR -0.87 *** PSMA4 pMN Mon 10 eGFR -0.87 *** PSMB9 pMN Mon 10 eGFR -0.86 ** PSME2 pMN Mon 10 eGFR -0.86 ** SAT1 pMN Mon 10 eGFR -0.71 * SFRS7 pMN cDC2 10 eGFR -0.86 ** SLC27A4 pMN cDC2 10 eGFR -0.70 * SLC35F1 pMN T 10 eGFR -0.80 ** B 10 eGFR -0.81 ** NK 10 eGFR -0.75 * Mon 10 eGFR -0.77 ** SLFN5 pMN NK 10 eGFR -0.80 ** TNFAIP3 pMN Mon 10 eGFR -0.79 ** TSC22D3 pMN cDC2 10 eGFR -0.71 *	MYO1F	pMN	cDC2	10	eGFR	0.79	**
PSMA4 pMN Mon 10 eGFR -0.77 ** PSMB9 pMN Mon 10 eGFR -0.87 ** PSME2 pMN Mon 10 eGFR -0.86 ** SAT1 pMN Mon 10 eGFR -0.71 * SFRS7 pMN cDC2 10 eGFR -0.86 ** SLC27A4 pMN cDC2 10 eGFR -0.70 * SLC35F1 pMN T 10 eGFR -0.80 ** B 10 eGFR -0.81 ** NK 10 eGFR -0.75 * Mon 10 eGFR -0.77 ** SLFN5 pMN NK 10 eGFR -0.80 ** TNFAIP3 pMN Mon 10 eGFR -0.79 ** TSC22D3 pMN cDC2 10 eGFR -0.71 * TYMP pMN Mon 10 eGFR -0.83 **	NFKBIA	pMN	В	10	eGFR	-0.64	*
PSMB9 pMN Mon 10 eGFR -0.87 ** PSME2 pMN Mon 10 eGFR -0.86 ** SAT1 pMN Mon 10 eGFR -0.71 * SFRS7 pMN cDC2 10 eGFR -0.86 ** SLC27A4 pMN cDC2 10 eGFR -0.70 * SLC35F1 pMN T 10 eGFR -0.80 ** B 10 eGFR -0.81 ** NK 10 eGFR -0.75 * Mon 10 eGFR -0.77 ** SLFN5 pMN NK 10 eGFR -0.80 ** TNFAIP3 pMN Mon 10 eGFR -0.79 ** TSC22D3 pMN cDC2 10 eGFR -0.71 * TYMP pMN Mon 10 eGFR -0.83 **	PDCD2	pMN	cDC2	10	eGFR	-0.87	***
PSME2 pMN Mon 10 eGFR -0.86 ** SAT1 pMN Mon 10 eGFR -0.71 * SFRS7 pMN cDC2 10 eGFR -0.86 ** SLC27A4 pMN cDC2 10 eGFR -0.80 ** SLC35F1 pMN T 10 eGFR -0.80 ** B 10 eGFR -0.81 ** NK 10 eGFR -0.75 * Mon 10 eGFR -0.77 ** SLFN5 pMN NK 10 eGFR -0.80 ** TNFAIP3 pMN Mon 10 eGFR -0.79 ** TSC22D3 pMN cDC2 10 eGFR -0.71 * TYMP pMN Mon 10 eGFR -0.83 **	PSMA4	pMN	Mon	10	eGFR	-0.77	**
SAT1 pMN Mon 10 eGFR -0.71 * SFRS7 pMN cDC2 10 eGFR -0.86 ** SLC27A4 pMN cDC2 10 eGFR -0.70 * SLC35F1 pMN T 10 eGFR -0.80 ** B 10 eGFR -0.81 ** NK 10 eGFR -0.75 * Mon 10 eGFR -0.80 ** TNFAIP3 pMN Mon 10 eGFR -0.79 ** TSC22D3 pMN cDC2 10 eGFR -0.81 ** TYMP pMN Mon 10 eGFR -0.71 *	PSMB9	pMN	Mon	10	eGFR	-0.87	**
SFRS7 pMN cDC2 10 eGFR -0.86 ** SLC27A4 pMN cDC2 10 eGFR -0.70 * SLC35F1 pMN T 10 eGFR -0.80 ** B 10 eGFR -0.81 ** NK 10 eGFR -0.75 * Mon 10 eGFR -0.80 ** TNFAIP3 pMN Mon 10 eGFR -0.79 ** TSC22D3 pMN cDC2 10 eGFR -0.81 * TYMP pMN Mon 10 eGFR -0.83 **	PSME2	pMN	Mon	10	eGFR	-0.86	**
SLC27A4 pMN cDC2 10 eGFR -0.70 * SLC35F1 pMN T 10 eGFR -0.81 ** B 10 eGFR -0.81 ** NK 10 eGFR -0.75 * Mon 10 eGFR -0.77 ** SLFN5 pMN NK 10 eGFR -0.80 ** TNFAIP3 pMN Mon 10 eGFR -0.79 ** TSC22D3 pMN cDC2 10 eGFR -0.71 * TYMP pMN Mon 10 eGFR -0.83 **	SAT1	pMN	Mon	10	eGFR	-0.71	*
SLC35F1 pMN T 10 eGFR -0.80 ** B 10 eGFR -0.81 ** NK 10 eGFR -0.75 * Mon 10 eGFR -0.77 ** SLFN5 pMN NK 10 eGFR -0.80 ** TNFAIP3 pMN Mon 10 eGFR -0.79 ** TSC22D3 pMN cDC2 10 eGFR -0.71 * TYMP pMN Mon 10 eGFR -0.83 **	SFRS7	pMN	cDC2	10	eGFR	-0.86	**
B 10 eGFR -0.81 ** NK 10 eGFR -0.75 * Mon 10 eGFR -0.77 ** SLFN5 pMN NK 10 eGFR -0.80 ** TNFAIP3 pMN Mon 10 eGFR -0.79 ** TSC22D3 pMN cDC2 10 eGFR -0.71 * TYMP pMN Mon 10 eGFR -0.83 **	SLC27A4	pMN	cDC2	10	eGFR	-0.70	*
NK 10 eGFR -0.75 * Mon 10 eGFR -0.77 ** SLFN5 pMN NK 10 eGFR -0.80 ** TNFAIP3 pMN Mon 10 eGFR -0.79 ** TSC22D3 pMN cDC2 10 eGFR -0.71 * TYMP pMN Mon 10 eGFR -0.83 **	SLC35F1	pMN	T	10	eGFR	-0.80	**
Mon 10 eGFR -0.77 ** SLFN5 pMN NK 10 eGFR -0.80 ** TNFAIP3 pMN Mon 10 eGFR -0.79 ** TSC22D3 pMN cDC2 10 eGFR -0.71 * TYMP pMN Mon 10 eGFR -0.83 **			В	10	eGFR	-0.81	**
SLFN5 pMN NK 10 eGFR -0.80 ** TNFAIP3 pMN Mon 10 eGFR -0.79 ** TSC22D3 pMN cDC2 10 eGFR -0.71 * TYMP pMN Mon 10 eGFR -0.83 **			NK	10	eGFR	-0.75	*
TNFAIP3 pMN Mon 10 eGFR -0.79 ** TSC22D3 pMN cDC2 10 eGFR -0.71 * TYMP pMN Mon 10 eGFR -0.83 **			Mon	10	eGFR	-0.77	**
TSC22D3 pMN cDC2 10 eGFR -0.71 * TYMP pMN Mon 10 eGFR -0.83 **	SLFN5	pMN	NK	10	eGFR	-0.80	**
TYMP pMN Mon 10 eGFR -0.83 **	TNFAIP3	pMN	Mon	10	eGFR	-0.79	**
TIME PIME MOIL TO COPE -0.83	TSC22D3	pMN	cDC2	10	eGFR	-0.71	*
WDR74 pMN cDC2 10 eGFR -0.72 *	TYMP	pMN	Mon	10	eGFR	-0.83	**
	WDR74	pMN	cDC2	10	eGFR	-0.72	*

pMN, primary membranous nephropathy; n, number of samples; eGFR, estimated glomerular filtration rate; R, correlation coefficient; *, p < 0.05; **, p < 0.01; ***, p < 0.001.

3.8 Abnormalities of Cell-Cell Communications in pMN

Prediction of intercellular communication networks is also necessary for figuring out the pathogenic mechanism of pMN. We analyzed potential cell-cell interactions by examining co-expression patterns of curated ligand-receptor pairs (Fig. 7A and Supplementary Fig. 7).

With regard to the relative information flow, we found that some interaction pairs increased significantly in disease groups, such as cell chemokines (*CCL*) and cytokines (*TGFB* and *IFN-II*) (Fig. 7A, **Supplementary** Fig. 7A,B,D). And many up-regulated pairs correlated with

functional changes in cell adhesion, such as *CD6*, *CD226*, *ALCAM*, *NECTIN* and *NCAM* (Fig. 7A) [37]. TIGIT-related pairs may facilitate the inhibition of monocytes by regulatory T cells, suggesting a protective mechanism that could prevent excessive monocyte-driven inflammation (Fig. 7A, **Supplementary Fig. 7C**) [38].

Conversely, information flow of some interaction pairs decreased remarkably in patients, such as human leukocyte antigen (HLA) molecules (major histocompatibility complex, class I and II) (Fig. 7A–C,E,F). All of the *HLA-I* molecules from PBMCs were decreased in patients compared to healthy donors (**Supplementary Fig. 6A–C**, Fig. 7H). Similar trends were showed in B cells for most of the *HLA-II* molecules (Fig. 7I,J). However, with regard to memory B cells, expression levels of *HLA-DQA1* and *HLA-DRB1* were significantly higher in patients (Fig. 7J–L). Overall, these findings suggest that memory B cells may play a role in the pathogenic mechanisms of pMN though HLA-DQA1 or HLA-DRB1 [39,40].

In addition, we found the putative CLEC2 (C-type lectin domain family 2) and KLRB1 (killer cell lectin like receptor B1) pairs were relatively activated in patients (Fig. 7A,D,G). Indeed, the expression levels of *CLEC2B*, CLEC2C (CD69) and CLEC2D in most cells were significantly upregulated in patients compared to healthy donors (Supplementary Fig. 6H) [41], as confirmed in CLEC score system (Supplementary Fig. 6I). KLRB1 was regarded as an inhibited receptors in CD56^{+/-} NK cells [42]. CLEC2B was expressed mainly in monocytes, T and NK cells, CLEC2C and CLEC2D were expressed prominently in T, B and NK cells (Supplementary Fig. 6H). We speculated that B and T cells might inhibit cytotoxic NK cells to prevent further kidney injury. This hypothesis was supported by decreased expression of granzyme M (GZMM) in NK (CD56+/-) cells (Supplementary Fig. **6C–G**). With regard to perforin 1 (*PRF1*) and *GZMB*, similar expression patterns were showed in NK (CD56+/-), Tem and Temra (CD8+) cells (Supplementary Fig. 6C). Furthermore, we found that index of cytotoxicity was significantly lower in patients than in healthy donors using our developed score (including GZMA, GZMB, GZMM, PRF1) (Supplementary Fig. 6G). Abnormal expression of Fc receptors in classical monocytes and cDC2 cells, such as FCAR and FCGR2B (Supplementary Fig. 6J-L), which may further disturb the antibody-dependent cell-mediated cytotoxicity [43,44]. Altogether, these finding suggests that the presence of a compensatory mechanism could mitigate glomerular injury.

4. Discussion

Membranous nephropathy is the most frequent cause of nephrotic syndrome in adults. Various kinds of autoantibodies have been identified in about 80–90% cases with MN. Patients with anti-PLA2R1 antibodies account for approximately 55% cases of total MN [45]. Recent studies



mapped the single-cell profile of kidney tissue from adult patients with pMN, which revealed functional abnormalities of impaired glomerulus and local microenvironment cells [5–8]. However, the immune pathogenic mechanism of pMN has been elusive until now, partly because of few immune cells in kidney biopsy tissues in these studies. One recent study reported the abnormalities of PBMCs from patients with untreated pMN. However, only three samples were involved in the study [9]. To our knowledge, our study is the first one to depict comprehensively the single-cell transcript profile of PBMCs from adult with newly-diagnosed pMN.

The immune complex deposits consist of immunoglobulin G and its related autoantigen PLA2R1 and complement components on the outer aspect of the basement membrane. It is not well known about the expression distribution of immunoglobulins in circulating B cells. Intriguingly, we found that expression levels of IGHG3 in memory B cells correlated positively with the severity of pMN, suggesting that IGHG3 is a good potential biomarker for distinguishing high-risk from moderate and low-risk patients with pMN [18]. More studies are required to explore the precise roles of IGHG3 in the development of pMN.

Persistent inflammation responses play a key role in many autoimmune diseases. We found that numerous inflammatory signalings were implicated into the development of pMN, including part members of interleulin, interferon, tumor necrosis factor, chemokine and growth factor families. As an upstream signaling, some pattern recognition receptor genes were up-regulated in patients. Similar trends were present with regard to some classical transcript factor signalings, such as MAPK, NF- κ B and JAK-STAT and AP-1 and so on [26–28,46]. Of course, it remains to be determined how the innate immune pathways mediate the initiation of pMN.

Unexpectedly, we discovered several novel biological processes in patients including cellular senescence, circadian rhythm and chromatin remodeling [29–32]. These conceptions have been proposed for decades. And they widely participated into the development of autoimmune disease and tumors. However, no relevant articles about pMN have been published until now, which implies that functional changes about peripheral-blood derived immune cells need to be explored comprehensively in near future.

In clinical practice, it is extremely important for doctors to distinguish high-risk patients from others effectively, which would contribute to the decision of treatment strategy. However, only few markers are used in practice, such as quantitative proteinuria and eGFR. In this study, we found that genes involved into the antiviral defense response in monocytes and lymphoid cells were elevated significantly in high-risk patients compared to low-risk population. The result suggests that unknown virus infections may play a critical role in the development of high-risk

pMN. Blocking the signaling pathway may do good to controlling the progression of high-risk pMN. Intriguingly, a large number of screened genes upregulated in high-risk patients correlated negatively with declined eGFP, such as SLC35F1 (solute carrier family 35 member F1) and BST2 (bone marrow stromal cell antigen 2). These biomarkers have a potential predictable value for assessing the severity of patients with newly-diagnosed pMN [36]. And we validated their predictable values in a larger population from a public database. Intriguingly, we found that peripheral blood cells have an equivalent role with kidney tissues for predicting the prognosis of kidney diseases. Additionally, we established a score system for distinguishing moderaterisk patients from low-risk and high-risk population.

Regarding cell-cell communication, multiple signaling pathways may contribute to the development of pMN, including antigen presentation, immune inhibition, cell adhesion and migration. First of all, all of the major histocompatibility complex (class I) molecules were significantly decreased in monocytes and lymphoid cells, implying that weakened interactions between HLA-I and CD8 might impair the antigen presentation of monocytes and NK cells to T (CD8+) cells. In terms of HLA-II and CD4 pairs, we found a significant upregulation of HLA-DQA1 and HLA-DRB1 in memory B cells in patients, indicating that the interactions between memory B and T (CD4+) cells might play a pivotal role in the pathogenesis of pMN [39,40]. Consistent with published articles, that the single nucleotide polymorphism (SNP) of HLA-DQA1 and HLA-DRB1 are associated with MN development. However, the relationship between SNP of HLA molecules and their expression levels requires further investigation. In addition, we discovered an increased interaction intensity of CLEC2-KLRB1 pairs in patients, suggesting function of NK cells may be suppressed by monocytes, T and B cells [41,42]. However, the direct interaction between CLEC2 and KLRB1 has yet to be confirmed through functional experiments. Further investigation is required to determine whether the inhibition of NK cells could potentially mitigate the progression of pMN.

A primary limitation of our study is that the findings need to be validated in a larger population. Additionally, we did not include healthy donors as a negative control group, which could have helped minimize batch effects between different datasets. To address this limitation, we utilized high-quality scRNA-seq data from a previously published study [11], where cryopreserved blood cells were thawed under conditions similar to ours. While this mitigates some variability, the lack of a dedicated negative control group remains a constraint. Another limitation is the inability to analyze single-cell profiles of kidney tissues from the same patients included in our study. This prevented a direct investigation of cell-cell communications between PBMCs and glomerulus-derived cells, which would have provided deeper insights into immune mechanisms and dis-



ease pathology. Furthermore, while our study employed various computational tools to analyze PBMC data, potential biases from cell clustering and annotation, as well as noise inherent to scRNA-seq data, may have slightly influenced the results. For example, the use of DoubletFinder may inadvertently remove some normal single cells that exhibit gene expression profiles similar to doublets. Such false negative results could reduce the number of effective cells used for further analysis. Another potential issue lies in the use of the Harmony algorithm for batch effect correction. This method is highly effective in aligning datasets and reducing technical variability, it may overcorrect batch effects in some cases, potentially masking genuine biological variations.

5. Conclusions

we conducted a comprehensive investigation into the immune profile of PBMCs from patients with pMN. Our findings indicate that antiviral defense response may play a critical role in the development of high-risk pMN. Furthermore, we identified numerous biomarkers capable of predicting declined eGFR in patients with pMN. These will give insight into the precise risk stratification of newly-diagnosed pMN and the optimization of current treatment strategies [4].

Abbreviations

ANOVA, analysis of variance; Ba, activated B cell; Bn, naive B cell; Bnsm, non-switched memory B cell; Bsm, switched memory B cell; CCL, chemokine; cDC2, classical dendritic cell 2; CR1, complement receptor 1; DEG, different expression gene; DMSO, dimethyl sulfoxide; eGFR, estimated glomerular filtration rate; ESRD, end-stage renal disease; GBM, glomerular basement membrane; GO, gene ontology; IgG4, immunoglobulin G4; IL1B, interleukin 1B; ILC3, innate lymphoid cell 3; IFNG, interferon G; Mc, classical monocyte; Mnc, non-classical monocyte; MAIT, mucosal-associated invariant T cell; NLR, NOD-like receptor; pMN, primary membranous nephropathy; PBMCs, peripheral blood mononuclear cells; PLA2R1, phospholipase A2 receptor 1; PRR, pattern recognition receptor; sMN, secondary membranous nephropathy; SNP, single nucleotide polymorphism; Tcm, central memory T cell; Te, effector T cell; Tem, effector memory T cell; Tn, naive T cell; Treg, regulatory T cell; TFs, transcript factor; TLR, toll-like receptor.

Availability of Data and Materials

The raw data of single-cell RNA sequencing from 11 patients with pMN during the current study are available in the Genome Sequence Archive for human (https://ngdc.cncb.ac.cn/gsa-human), under the accession number: PRJCA033292 (the datasets will be available to the public once the manuscript in press). The raw data from

5 healthy donors are publicly available in the NCBI GEO database (GSE158055).

Author Contributions

XLS, LHW, and XQ designed the study. XT and SLY performed experiments; ZAC and XT performed statistical analyses. BXW, BJY and HFZ facilitated participant recruitment and sample collection. XT wrote the manuscript. XLS contributed to funding acquisition for the study. All authors reviewed and approved the final manuscript. All authors contributed to editorial changes in the manuscript. All authors have participated sufficiently in the work and agreed to be accountable for all aspects of the work.

Ethics Approval and Consent to Participate

The study was carried out in accordance with the guidelines of the Declaration of Helsinki. The study protocols were approved by the Ethics Committees of the Second Hospital of Shanxi Medical University in China (NO. 2024YX379). All the patients or their families/legal guardians in our study were provided written informed consent.

Acknowledgment

The authors thank all participants. We thank the Zhejiang Puluoting Health Technology Company for providing single-cell RNA sequencing.

Funding

This work was supported by grants from Shanxi Province Health Commission Science Fund (2022002) and "Yiluqihang & Shenmingyuanyang" Medical Development and Scientific Research Fund project on kidney diseases (SMYY20220301001).

Conflict of Interest

The authors declare no conflict of interest. Despite receiving sponsorship from Zhejiang Puluoting Health Technology Company, the judgments in data interpretation and writing were not influenced by this relationship.

Supplementary Material

Supplementary material associated with this article can be found, in the online version, at https://doi.org/10.31083/FBL36332.

References

- [1] Hoxha E, Reinhard L, Stahl RAK. Membranous nephropathy: new pathogenic mechanisms and their clinical implications. Nature Reviews. Nephrology. 2022; 18: 466–478. https://doi.org/10.1038/s41581-022-00564-1.
- [2] Ronco P, Beck L, Debiec H, Fervenza FC, Hou FF, Jha V, *et al*. Membranous nephropathy. Nature Reviews. Disease Primers. 2021; 7: 69. https://doi.org/10.1038/s41572-021-00303-z.



- [3] Avasare R, Andeen N, Beck L. Novel Antigens and Clinical Updates in Membranous Nephropathy. Annual Review of Medicine. 2024; 75: 219–332. https://doi.org/10.1146/annurev-med-050522-034537.
- [4] Fervenza FC, Appel GB, Barbour SJ, Rovin BH, Lafayette RA, Aslam N, et al. Rituximab or Cyclosporine in the Treatment of Membranous Nephropathy. The New England Journal of Medicine. 2019; 381: 36–46. https://doi.org/10.1056/NEJMoa 1814427.
- [5] Xu J, Shen C, Lin W, Meng T, Ooi JD, Eggenhuizen PJ, et al. Single-Cell Profiling Reveals Transcriptional Signatures and Cell-Cell Crosstalk in Anti-PLA2R Positive Idiopathic Membranous Nephropathy Patients. Frontiers in Immunology. 2021; 12: 683330. https://doi.org/10.3389/fimmu.2021.683330.
- [6] Yu L, Lin W, Shen C, Meng T, Jin P, Ding X, et al. Intrarenal Single-Cell Sequencing of Hepatitis B Virus Associated Membranous Nephropathy. Frontiers in Medicine. 2022; 9: 869284. https://doi.org/10.3389/fmed.2022.869284.
- [7] Shi M, Wang Y, Zhang H, Ling Z, Chen X, Wang C, et al. Single-cell RNA sequencing shows the immune cell landscape in the kidneys of patients with idiopathic membranous nephropathy. Frontiers in Immunology. 2023; 14: 1203062. https://doi.org/10.3389/fimmu.2023.1203062.
- [8] Feng X, Chen Q, Zhong J, Yu S, Wang Y, Jiang Y, et al. Molecular characteristics of circulating B cells and kidney cells at the single-cell level in special types of primary membranous nephropathy. Clinical Kidney Journal. 2023; 16: 2639–2651. https://doi.org/10.1093/ckj/sfad215.
- [9] Gu Q, Wen Y, Cheng X, Qi Y, Cao X, Gao X, et al. Integrative profiling of untreated primary membranous nephropathy at the single-cell transcriptome level. Clinical Kidney Journal. 2024; 17: sfae168. https://doi.org/10.1093/ckj/sfae168.
- [10] Rovin BH, Adler SG, Barratt J, Bridoux F, Burdge KA, Chan TM, et al. Executive summary of the KDIGO 2021 Guideline for the Management of Glomerular Diseases. Kidney International. 2021; 100: 753–779. https://doi.org/10.1016/j.kint.2021.05.015.
- [11] Ren X, Wen W, Fan X, Hou W, Su B, Cai P, *et al.* COVID-19 immune features revealed by a large-scale single-cell transcriptome atlas. Cell. 2021; 184: 1895–1913.e19. https://doi.org/10.1016/j.cell.2021.01.053.
- [12] Andrews TS, Kiselev VY, McCarthy D, Hemberg M. Tutorial: guidelines for the computational analysis of single-cell RNA sequencing data. Nature Protocols. 2021; 16: 1–9. https://doi.org/ 10.1038/s41596-020-00409-w.
- [13] Stuart T, Butler A, Hoffman P, Hafemeister C, Papalexi E, Mauck WM, 3rd, et al. Comprehensive Integration of Single-Cell Data. Cell. 2019; 177: 1888–1902.e21. https://doi.org/10. 1016/j.cell.2019.05.031.
- [14] Hao Y, Hao S, Andersen-Nissen E, Mauck WM, 3rd, Zheng S, Butler A, et al. Integrated analysis of multimodal single-cell data. Cell. 2021; 184: 3573–3587.e29. https://doi.org/10.1016/ j.cell.2021.04.048.
- [15] Korsunsky I, Millard N, Fan J, Slowikowski K, Zhang F, Wei K, et al. Fast, sensitive and accurate integration of single-cell data with Harmony. Nature Methods. 2019; 16: 1289–1296. https://doi.org/10.1038/s41592-019-0619-0.
- [16] Domínguez Conde C, Xu C, Jarvis LB, Rainbow DB, Wells SB, Gomes T, *et al*. Cross-tissue immune cell analysis reveals tissue-specific features in humans. Science (New York, N.Y.). 2022; 376: eabl5197. https://doi.org/10.1126/science.abl5197.
- [17] Jin S, Guerrero-Juarez CF, Zhang L, Chang I, Ramos R, Kuan CH, *et al.* Inference and analysis of cell-cell communication using CellChat. Nature Communications. 2021; 12: 1088. https://doi.org/10.1038/s41467-021-21246-9.
- [18] Seifert L, Zahner G, Meyer-Schwesinger C, Hickstein N,

- Dehde S, Wulf S, *et al.* The classical pathway triggers pathogenic complement activation in membranous nephropathy. Nature Communications. 2023; 14: 473. https://doi.org/10.1038/s41467-023-36068-0.
- [19] Furman D, Campisi J, Verdin E, Carrera-Bastos P, Targ S, Franceschi C, et al. Chronic inflammation in the etiology of disease across the life span. Nature Medicine. 2019; 25: 1822– 1832. https://doi.org/10.1038/s41591-019-0675-0.
- [20] Wang S, Diao H, Guan Q, Cruikshank WW, Delovitch TL, Jevnikar AM, et al. Decreased renal ischemia-reperfusion injury by IL-16 inactivation. Kidney International. 2008; 73: 318–326. https://doi.org/10.1038/sj.ki.5002692.
- [21] Gong T, Liu L, Jiang W, Zhou R. DAMP-sensing receptors in sterile inflammation and inflammatory diseases. Nature Reviews. Immunology. 2020; 20: 95–112. https://doi.org/10.1038/ s41577-019-0215-7.
- [22] Fillatreau S, Manfroi B, Dörner T. Toll-like receptor signalling in B cells during systemic lupus erythematosus. Nature Reviews. Rheumatology. 2021; 17: 98–108. https://doi.org/10. 1038/s41584-020-00544-4.
- [23] Chou WC, Jha S, Linhoff MW, Ting JPY. The NLR gene family: from discovery to present day. Nature Reviews. Immunology. 2023; 23: 635–654. https://doi.org/10.1038/ s41577-023-00849-x.
- [24] Rehwinkel J, Gack MU. RIG-I-like receptors: their regulation and roles in RNA sensing. Nature Reviews. Immunology. 2020; 20: 537–551. https://doi.org/10.1038/s41577-020-0288-3.
- [25] Zhang X, Bai XC, Chen ZJ. Structures and Mechanisms in the cGAS-STING Innate Immunity Pathway. Immunity. 2020; 53: 43–53. https://doi.org/10.1016/j.immuni.2020.05.013.
- [26] Arthur JSC, Ley SC. Mitogen-activated protein kinases in innate immunity. Nature Reviews. Immunology. 2013; 13: 679–692. https://doi.org/10.1038/nri3495.
- [27] Sun SC. The non-canonical NF-κB pathway in immunity and inflammation. Nature Reviews. Immunology. 2017; 17: 545– 558. https://doi.org/10.1038/nri.2017.52.
- [28] Dai D, Gu S, Han X, Ding H, Jiang Y, Zhang X, et al. The transcription factor ZEB2 drives the formation of age-associated B cells. Science (New York, N.Y.). 2024; 383: 413–421. https://doi.org/10.1126/science.adf8531.
- [29] Huang W, Hickson LJ, Eirin A, Kirkland JL, Lerman LO. Cellular senescence: the good, the bad and the unknown. Nature Reviews. Nephrology. 2022; 18: 611–627. https://doi.org/10.1038/s41581-022-00601-z.
- [30] Costello HM, Johnston JG, Juffre A, Crislip GR, Gumz ML. Circadian clocks of the kidney: function, mechanism, and regulation. Physiological Reviews. 2022; 102: 1669–1701. https://doi.org/10.1152/physrev.00045.2021.
- [31] Wolf BK, Zhao Y, McCray A, Hawk WH, Deary LT, Sugiarto NW, et al. Cooperation of chromatin remodeling SWI/SNF complex and pioneer factor AP-1 shapes 3D enhancer landscapes. Nature Structural & Molecular Biology. 2023; 30: 10– 21. https://doi.org/10.1038/s41594-022-00880-x.
- [32] Fortin BM, Pfeiffer SM, Insua-Rodríguez J, Alshetaiwi H, Moshensky A, Song WA, et al. Circadian control of tumor immunosuppression affects efficacy of immune checkpoint blockade. Nature Immunology. 2024; 25: 1257–1269. https://doi.org/ 10.1038/s41590-024-01859-0.
- [33] Diebold M, Locher E, Boide P, Enzler-Tschudy A, Faivre A, Fischer I, et al. Incidence of new onset glomerulonephritis after SARS-CoV-2 mRNA vaccination is not increased. Kidney International. 2022; 102: 1409–1419. https://doi.org/10.1016/j.kint.2022.08.021.
- [34] Li L, Fu L, Zhang L, Feng Y. Varicella-zoster virus infection and primary membranous nephropathy: a Mendelian randomization study. Scientific Reports. 2023; 13: 19212. https://doi.org/10.



- 1038/s41598-023-46517-x.
- [35] Atikuzzaman M, Alvarez-Rodriguez M, Vicente-Carrillo A, Johnsson M, Wright D, Rodriguez-Martinez H. Conserved gene expression in sperm reservoirs between birds and mammals in response to mating. BMC Genomics. 2017; 18: 98. https://doi. org/10.1186/s12864-017-3488-x.
- [36] Di Fede E, Peron A, Colombo EA, Gervasini C, Vignoli A. SLC35F1 as a candidate gene for neurodevelopmental disorders resembling Rett syndrome. American Journal of Medical Genetics. Part a. 2021; 185: 2238–2240. https://doi.org/10.1002/ajmg.a.62203.
- [37] Chalmers SA, Ramachandran RA, Garcia SJ, Der E, Herlitz L, Ampudia J, *et al.* The CD6/ALCAM pathway promotes lupus nephritis via T cell–mediated responses. The Journal of Clinical Investigation. 2022; 132: e147334. https://doi.org/10.1172/JC I147334.
- [38] Banta KL, Xu X, Chitre AS, Au-Yeung A, Takahashi C, O'Gorman WE, et al. Mechanistic convergence of the TIGIT and PD-1 inhibitory pathways necessitates co-blockade to optimize anti-tumor CD8+ T cell responses. Immunity. 2022; 55: 512–526.e9. https://doi.org/10.1016/j.immuni.2022.02.005.
- [39] Stanescu HC, Arcos-Burgos M, Medlar A, Bockenhauer D, Kottgen A, Dragomirescu L, et al. Risk HLA-DQA1 and PLA(2)R1 alleles in idiopathic membranous nephropathy. The New England Journal of Medicine. 2011; 364: 616–626. https://doi.org/10.1056/NEJMoa1009742.
- [40] Xie J, Liu L, Mladkova N, Li Y, Ren H, Wang W, et al. The genetic architecture of membranous nephropathy and its potential to improve non-invasive diagnosis. Nature Communications.

- 2020; 11: 1600. https://doi.org/10.1038/s41467-020-15383-w.
- [41] Herzog BH, Fu J, Wilson SJ, Hess PR, Sen A, McDaniel JM, et al. Podoplanin maintains high endothelial venule integrity by interacting with platelet CLEC-2. Nature. 2013; 502: 105–109. https://doi.org/10.1038/nature12501.
- [42] Sun Y, Wu L, Zhong Y, Zhou K, Hou Y, Wang Z, *et al.* Single-cell landscape of the ecosystem in early-relapse hepatocellular carcinoma. Cell. 2021; 184: 404–421.e16. https://doi.org/10.1016/j.cell.2020.11.041.
- [43] Jonsson S, Sveinbjornsson G, de Lapuente Portilla AL, Swaminathan B, Plomp R, Dekkers G, *et al.* Identification of sequence variants influencing immunoglobulin levels. Nature Genetics. 2017; 49: 1182–1191. https://doi.org/10.1038/ng.3897.
- [44] Wu X, Azizan EAB, Goodchild E, Garg S, Hagiyama M, Cabrera CP, et al. Somatic mutations of CADM1 in aldosterone-producing adenomas and gap junction-dependent regulation of aldosterone production. Nature Genetics. 2023; 55: 1009–1021. https://doi.org/10.1038/s41588-023-01403-0.
- [45] Sethi S, Beck LH, Jr, Glassock RJ, Haas M, De Vriese AS, Caza TN, et al. Mayo Clinic consensus report on membranous nephropathy: proposal for a novel classification. Kidney International. 2023; 104: 1092–1102. https://doi.org/10.1016/j.kint .2023.06.032.
- [46] Zhao Q, Dai H, Jiang H, Zhang N, Hou F, Zheng Y, et al. Activation of the IL-6/STAT3 pathway contributes to the pathogenesis of membranous nephropathy and is a target for Mahuang Fuzi and Shenzhuo Decoction (MFSD) to repair podocyte damage. Biomedicine & Pharmacotherapy. 2024; 174: 116583. https://doi.org/10.1016/j.biopha.2024.116583.

